

2F

---

# **Evaluation of Synroc-C as a Second-Generation Waste Form**

**J. W. Shade**

---

**August 1986**

**Prepared for the U.S. Department of Energy  
under Contract DE-AC06-76RLO 1830**

**Pacific Northwest Laboratory  
Operated for the U.S. Department of Energy  
by Battelle Memorial Institute**



## DISCLAIMER

This report was prepared as an account of work sponsored by an agency of the United States Government. Neither the United States Government nor any agency thereof, nor any of their employees, makes any warranty, express or implied, or assumes any legal liability or responsibility for the accuracy, completeness, or usefulness of any information, apparatus, product, or process disclosed, or represents that its use would not infringe privately owned rights. Reference herein to any specific commercial product, process, or service by trade name, trademark, manufacturer, or otherwise, does not necessarily constitute or imply its endorsement, recommendation, or favoring by the United States Government or any agency thereof. The views and opinions of authors expressed herein do not necessarily state or reflect those of the United States Government or any agency thereof.

PACIFIC NORTHWEST LABORATORY  
*operated by*  
BATTELLE  
*for the*  
UNITED STATES DEPARTMENT OF ENERGY  
*under Contract DE-AC06-76RLO 1830*

Printed in the United States of America  
Available from  
National Technical Information Service  
United States Department of Commerce  
5285 Port Royal Road  
Springfield, Virginia 22161

NTIS Price Codes  
Microfiche A01

### Printed Copy

Pages	Price Codes
001-025	A02
026-050	A03
051-075	A04
076-100	A05
101-125	A06
126-150	A07
151-175	A08
176-200	A09
201-225	A010
226-250	A011
251-275	A012
276-300	A013

EVALUATION OF SYNROC-C AS A  
SECOND-GENERATION WASTE FORM

J. W. Shade

August 1986

Prepared for  
the U.S. Department of Energy  
under Contract DE-AC06-76RLO 1830

Pacific Northwest Laboratory  
Richland, Washington 99352



## ABSTRACT

The durability of a crystalline titanate waste form, Synroc-C, was evaluated as a second-generation waste form by leach testing. Tests using both monolith and high surface area powdered samples were used with silicate water and brines at 90°C and 150°C for up to 90 days. In addition, low surface area-to-volume ratio, 1-day leach tests were conducted between 90°C and 250°C to determine forward-direction leach rates and activation energies. Dissolution rates of Cs, Mo, Ba, and U indicated that Synroc-C generally performed about an order of magnitude better than uranium-doped 76-68 glass. The release of Cs and Mo from Synroc-C, at least initially, may be primarily from intergranular regions of the material. The activation energy for the release of these elements from glass was about 9 kcal/mol but less than 3 kcal/mol for Synroc-C. In long-term tests, uranium dissolution may be controlled more by the formation of uranium alteration products than by release from the waste form.



## SUMMARY

Both glass and crystalline ceramic materials are being considered as waste containment forms for nuclear fuel reprocessing wastes and are under consideration along with unprocessed spent fuel for disposal in geologic repositories. Although borosilicate glasses have received the most development effort in the past, high-temperature glasses, glass-ceramics, and crystalline ceramics are presently under consideration as second-generation waste forms. The crystalline titanate ceramic Synroc, among others, has exhibited good performance as a candidate second-generation waste form.

The purpose of this study was to evaluate the leaching performance of an Australian-prepared Synroc-C (for commercial waste) by comparison with a well-documented borosilicate glass, MCC 76-68, using several test methods. The selection of leach tests was intended to focus on measurements, such as saturation values and initial leach rates, that can be applied to repository transport models as well as be used to compare waste forms.

The 76-68 glass used in this work contained 33 wt% PW-8a waste calcine and 4.16 wt% UO<sub>2</sub>, while the Synroc-C contained 10 wt% PW-4b calcine and 0.49 wt% UO<sub>2</sub>. Uranium was the only radioactive species in these tests. Two test procedures were used: a modified MCC-1 procedure using monolithic test specimens and the MCC-3 procedure using specimens crushed to -40/+80 mesh (-420/+177 μm) to obtain an unreacted high surface area. The tests were conducted at 90°C and 150°C in silicate water (0.002 M NaHCO<sub>3</sub>, 0.001 M SiO<sub>2</sub>) with a pH of 8.67 and brine (0.65 M KCl, 1.54 M NaCl, 1.22 M MgCl<sub>2</sub>) with a pH of 4.43. The monolith tests were terminated at 28 days, but the MCC-3 powder tests were continued for up to 90 days. All leachate samples were filtered through 0.5-μm filters, and samples from powder tests were also filtered through 1.8-nm filters to determine possible colloidal species. In addition to these tests, the temperature dependence on the initial leach rate was estimated between 90°C and 250°C in low surface area-to-volume (SA/V) tests conducted for 1 day.

The performance of Synroc-C relative to 76-68 glass in silicate water can be considered in terms of the release of Ba, Mo, Cs, and U. In monolith tests for up to 28 days, Ba concentrations found in solution from Synroc were less

than 1 ppm at 90°C and increased by about a factor of three at 150°C. Ba is present in glass only as an impurity, and dissolution rates are consequently less than in Synroc. The concentrations of Mo, Cs, and U in these monolith tests were normalized to the amount present in the waste form material. Normalized Mo released from Synroc ( $2.0 \text{ g/m}^2$ ) was about an order of magnitude lower than from glass at 90°C. At 150°C, however, normalized Mo was more than an order of magnitude higher in glass systems than in Synroc and indicated little temperature effect. Normalized Cs also showed very little temperature effect for Synroc with values of about  $0.3 \text{ g/m}^2$ , but Cs concentrations from glass systems were  $20 \text{ g/m}^2$  at 90°C and  $80 \text{ g/m}^2$  at 150°C. At 90°C, normalized U concentrations were about  $5.0 \text{ g/m}^2$  from glass monoliths but were about  $0.1 \text{ g/m}^2$  for Synroc. At 150°C, limited data suggest that normalized U concentrations for Synroc may approach those for glass.

Results from the powder leach tests are reported in terms of concentrations, not normalized with respect to the amount present in the waste form material. U concentrations reached a maximum at 28 days and decreased to less than 10 ppb for both Synroc and glass at 90 days, suggesting that a similar U-bearing reaction product may be forming for both materials. Comparisons of 0.5- $\mu\text{m}$  and 1.8-nm filtrates indicated that part of the U from glass may form colloids and that Ba from Synroc also tends to form small particles. Concentrations of Ba in silicate water at 90°C were near 5 ppm in 0.5- $\mu\text{m}$  filtrates but were about 1 ppm in 1.8-nm filtrates. Cs concentrations approached a steady state of about 10 ppm in glass systems but were about an order of magnitude lower in Synroc systems, suggesting that two different Cs phases are controlling dissolution. The Mo concentration reached a steady-state value of 10 ppm in Synroc powder tests at 90 days, but Mo release from glass was about a factor of five higher and did not exhibit steady-state behavior.

The temperature dependence for the initial release rate of Mo and Cs was estimated for both waste forms between 90°C and 250°C by conducting 1-day dissolution tests at low SA/V ratios. In glass systems, initial release rates were one to three orders of magnitude higher than in Synroc. Activation energies determined from Cs release rates from glass were the same as those

from Mo and had a value of 8.7 kcal/mol, ignoring some slight curvature in the data. Activation energies determined from Cs release rates from Synroc were 3.2 kcal/mol while those based on Mo release were about 1.3 kcal/mol, suggesting that Cs and Mo are associated with separate phases in Synroc.

In conclusion, Synroc-C appears to have about one order of magnitude better performance than a 76-68-type borosilicate glass, based on general leach test data. The concentrations of some radionuclides that typically form low solubility reaction products, such as uranium, may be controlled more by the type of reaction product formed than by release from waste forms.



## CONTENTS

ABSTRACT .....	iii
SUMMARY .....	v
INTRODUCTION .....	1
CONCLUSIONS .....	3
SELECTION OF LEACH TESTS .....	5
EXPERIMENTAL METHODS .....	9
RESULTS AND DISCUSSION .....	13
SILICATE WATER LEACH TEST RESULTS .....	13
BRINE LEACH TEST RESULTS .....	26
REFERENCES .....	29
APPENDIX A - LEACH TEST RESULTS FROM MCC-1 AND MCC-2 TESTS ON SYNROC-C AND 76-68 GLASS IN SILICATE WATER .....	A.1
APPENDIX B - LEACH TEST RESULTS FROM MCC-1 AND MCC-2 TESTS ON SYNROC-C AND 76-68 GLASS IN BRINE .....	B.1
APPENDIX C - LEACH TEST RESULTS FROM MCC-3 TESTS ON SYNROC-C AND 76-68 GLASS IN SILICATE WATER .....	C.1
APPENDIX D - LEACH TEST RESULTS FROM MCC-3 TESTS ON SYNROC-C AND 76-68 GLASS IN BRINE .....	D.1

## FIGURES

1	Final pH Values from Silicate Water Tests with Powders at 90°C and 150°C .....	15
2	Ba Concentrations for Synroc-C and 76-68 Glass Monoliths in Silicate Water at 90°C and 150°C .....	15
3	Normalized Cs Dissolution from Synroc-C and 76-68 Glass Monoliths in Silicate Water Tests at 90°C and 150°C .....	16
4	Normalized Mo Dissolution from Synroc-C and 76-68 Glass Monoliths in Silicate Water Tests at 90°C and 150°C .....	16
5	Normalized U Dissolution from Synroc-C and 76-68 Glass Monoliths in Silicate Water Tests at 90°C and 150°C .....	17
6	Ba, Cs, and Mo Concentrations in 0.5- $\mu$ m and 1.8-nm Filtrates of Silicate Water from Synroc-C Powder Tests at 90°C .....	18
7	Ba, Cs, and Mo Concentrations for Synroc-C and 76-68 Glass Powders in 0.5- $\mu$ m Filtrates of Silicate Water at 90°C .....	18
8	U Concentrations from 0.5- $\mu$ m and 1.8-nm Filtrates of Synroc-C and 76-68 Powders in Silicate Water at 90°C .....	19
9	Cs Concentrations in 0.5 $\mu$ m Filtrates from Monolith and Powder Tests for Synroc-C and 76-68 Glass in Silicate Water at 90°C .....	21
10	Mo Concentrations in 0.5- $\mu$ m Filtrates from Monolith and Powder Tests for Synroc-C and 76-68 Glass in Silicate Water at 90°C .....	21
11	Mo Concentrations in 0.5- $\mu$ m Filtrates from Monolith and Powder Tests for Synroc-C and 76-68 Glass in Silicate Water at 150°C .....	22
12	Cs Concentrations in 0.5- $\mu$ m Filtrates from Monolith and Powder Tests for Synroc-C and 76-68 Glass in Silicate Water at 150°C .....	22
13	Temperature Dependence of Mo and Cs Forward Dissolution Rates Between 90°C and 250°C for Synroc-C and 76-68 Glass in Silicate Water .....	25

TABLES

1	Compositions of U-Doped 76-68 Glass and Synroc-C .....	10
2	Leachate Composition Changes Due to Sorption on Container Walls .....	12
3	MCC-1 and MCC-2 Brine Leach Data .....	27
4	MCC-3 Brine Leach Data .....	27



## INTRODUCTION

Both glass and crystalline ceramic materials are being developed as waste containment forms for nuclear fuel reprocessing wastes and are under consideration along with unprocessed spent fuel for disposal in geologic repositories. Excluding direct disposal of unprocessed spent fuel (which is also being considered as a viable waste form), glass has been developed to the greatest extent as a high-level nuclear waste form, while ceramic materials have received less attention. Over the last 15 years, several types of ceramic waste forms such as supercalcine, Synroc, and various glass-ceramics have been investigated as alternatives to glass (Casey 1978; Chikalla and Mendel 1979). Some of these materials are being reconsidered as second-generation waste forms because they show promise of having better leaching and corrosion resistance than current waste forms.

The leaching behavior of a Synroc composition designated Synroc-C (supplied by the Australia Atomic Energy Commission) is evaluated in this report as a possible second-generation waste form. These results can be compared with results from leach tests on other second-generation waste form candidates such as high alumina glass (Bunnell, Maupin, and Oma 1986) and sphene glass-ceramics (Hayward et al. 1986). This evaluation was conducted by Pacific Northwest Laboratory (PNL)<sup>(a)</sup> under the Nuclear Waste Treatment Program.

The general concept of radionuclide containment by crystalline ceramic waste forms involves a choice of crystalline phases capable of accommodating long-lived radionuclides in durable crystalline phases that have low solubility products. Because reprocessing waste streams are chemically complex, it is necessary that crystalline structures be relatively open so that several kinds of ions representing a moderate range of ionic radii and ionic charge can be contained as solid solution components. For fabrication purposes, waste loadings, and phase stability, it is also desirable that the number of phases remain low. Thus, most ceramic waste forms are based on three to five silicate or titanate phases that have very low reactivity with repository environments.

---

(a) Operated for the U.S. Department of Energy under Contract DE-AC06-76RLO 1830.

For example, supercalcine is a silicate-based waste form (McCarthy and Davidson 1975), while Synroc-C is a titanate-based waste form (Ringwood 1978). Unless a glass-ceramic is specifically desired, fabrication methods for ceramic waste forms are generally directed towards producing nearly complete crystallinity in products that approach theoretical density as closely as possible.

In contrast to ceramic waste forms, isolation of radionuclides in glass structures is based on the ability of a structurally flexible glass network to contain the complete size range of radionuclides present in waste streams in a single matrix. In an idealized crystalline phase, a given radionuclide contained in a specific crystallographic site with highly directional bonding would be energetically more stable than the same radionuclide distributed in two or more sites, possibly including interstitial sites, in a random glass network. This kind of reasoning has led to continued investigation of ceramic waste forms because their potential durability may exceed that of glass.

The structural differences between glass and crystalline ceramic waste forms as well as the differences in waste loading and radionuclide containment concepts require that appropriate methods of waste form evaluation be selected to insure equitable comparison. Differences in matrix dissolution mechanisms between crystalline and glass materials of the same composition may also affect leach model development (Shade 1981). Leach tests conducted during waste form development are typically short-term tests that compare release rates of elements normalized to the waste form composition. This approach may be appropriate for ranking waste form compositions within a single waste form type (such as glass) but may not be adequate to characterize diverse types of waste forms representing broad ranges in waste loadings. Moreover, the release rate of elements from a waste form is only one parameter required for evaluating waste forms in a repository environment and may not be as important as other factors, some site-related, such as molecular diffusivity, groundwater flow rate, or the presence of colloid-forming components from the waste package system and repository rock (Zavoshy, Chambre, and Pigford 1985).

## CONCLUSIONS

The following conclusions are based on the results of leach tests of Synroc-C and 76-68 glass:

- The dissolution rates of comparable elements such as Cs and Mo from Synroc-C are about an order of magnitude less than from 76-68 glass.
- A probable source of elements leached from Synroc-C is from an intergranular amorphous phase rather than crystalline phases.
- Elements such as Cs and Mo reach saturation as a function of the surface-area-to-volume (SA/V) ratio more rapidly for Synroc samples than for glass. The activation energies associated with dissolution of these elements from Synroc are also low.
- The relative leaching behavior of Synroc-C with respect to 76-68 glass in brines is about the same as in silicate water, which is usually about an order of magnitude difference in concentration for comparable elements such as Cs and Mo.
- Uranium dissolution from Synroc-C and 76-68 glass may be controlled more by the formation of reaction products than by dissolution rates from waste forms.



## SELECTION OF LEACH TESTS

The selection of an appropriate series of leach tests to evaluate Synroc-C was based on a desire to recognize waste form interactions with repository components and to provide measurements applicable to current radionuclide transport models. It was also desired to utilize some of the leach test methods developed by the Materials Characterization Center (MCC). Accordingly, modified versions of MCC-1 (MCC 1981) and MCC-3 (MCC 1984), using monolithic and powdered tests specimens, respectively, were selected along with an additional test designed to determine the forward-direction leach rate and the temperature dependence on the forward rate. To at least symbolically recognize repository interactions, only two of the three MCC solutions (MCC 1981) were used as leachates: a low-ionic-strength sodium bicarbonate ( $0.002 \text{ M NaHCO}_3$ )-silicate ( $0.001 \text{ M SiO}_2$ ) solution and a brine ( $0.65 \text{ M KCl}$ ,  $1.54 \text{ M NaCl}$ ,  $1.22 \text{ M MgCl}_2$ ). The third MCC solution, deionized water, was not used. The silicate water was used to represent groundwater water types associated with crystalline aluminosilicate rock environments; the brine is a simplified representative of fluids from salt formations.

The results from these types of tests can be used to evaluate waste forms in terms of transport models developed to predict radionuclide migration rates in repository systems. One such model assumes that elements released from waste forms become saturated in a narrow zone adjacent to the waste form or at the waste form surface and that transport is limited by molecular diffusion in a low flow system (Chambre, Zavoshy, and Pigford 1982). Saturation values, such as might be expected from high SA/V ratio powder tests (MCC-3), are required for this model.

In an extension of this model (Zavoshy, Chambre, and Pigford 1985), two processes were considered. In one case, dissolved waste components migrate away from the waste form surface faster than the dissolution rate; thus, saturation is not attained. This situation might occur in a relatively fast flowing system and has been referred to as a surface-reaction-controlled

process (Berner 1978). The rate-limiting step in this case is the forward dissolution rate, which is generally assumed to be first order with respect to matrix elements.

In the other case, radionuclide transport is limited by molecular diffusion of dissolved components away from the surface of the waste form or by diffusion plus convection in a flowing system. Dissolved components become saturated at the waste form surface and their release rate is referred to as transport controlled (Berner 1978).

To determine which of these two processes may be dominant in a given system, a "flux ratio," R, has been defined as follows (Zavoshy, Chambre, and Pigford 1985):

$$R = \frac{\text{Forward dissolution rate per unit area}}{\text{Diffusive/convective mass transfer rate}}$$

When R is less than 1, the dissolved components migrate away from the waste form surface faster than they can be replenished by dissolution so that saturation is not attained and the system is surface reaction controlled. This situation would be expected where the groundwater flow rate exceeds the dissolution rate of components from the waste form. When R is greater than 1, probably a more likely case, concentrations of dissolved components are at saturation and the release rate becomes transport controlled. This situation could occur under low flow rates or near static conditions.

The following analytical expression for the flux ratio has been derived (Zavoshy, Chambre, and Pigford 1985):

$$R = \frac{(J_0) (r_0)}{(e) (D) (C_s)}$$

where  $J_0$  = forward dissolution rate

$r_0$  = waste form radius

$e$  = porosity of the surrounding medium

$D$  = liquid diffusion coefficient

$C_s$  = saturation value (or solubility) of a component.

This transport model utilizes relative values of waste form dissolution rates and groundwater flow rates to evaluate controls on waste form dissolution. The required variables for determining which of these two rates are dominant are contained in the expression for the flux ratio. Two of these variables, the forward dissolution rate ( $J_0$ ) and the saturation value ( $C_s$ ) can be obtained from an appropriate choice of waste form dissolution tests. This concept has served as the basis for the choice of tests used in this work, which emphasize attempts to experimentally evaluate  $J_0$  and  $C_s$ . In addition, activation energies obtained from the temperature dependence of  $J_0$  will be used to provide an indication of the overall capability of materials to retain components.



## EXPERIMENTAL METHODS

The bulk compositions of U-doped 76-68 glass (ATM-1; Mellinger and Daniel 1984) and Synroc-C<sup>(a)</sup> are compared in Table 1. The glass composition differs from Synroc-C both in terms of waste loading and in the type of calcine used to prepare the simulated waste. The 76-68 glass contained 33 wt% PW-8a waste calcine and 4.16 wt% depleted UO<sub>2</sub>; the Synroc-C contained 10 wt% PW-4b waste calcine and 0.49 wt% UO<sub>2</sub>. The Synroc-C was supplied as a large 500-g pellet, cut in half; and the glass was obtained in the form of bars. Test materials were prepared from these sources using methods described in the MCC-1 and MCC-3 test procedures (MCC 1981, 1984).

Monolith specimens were prepared by cutting small wafers, about 1 to 4 cm<sup>2</sup> in surface area, using a diamond saw with water as the cutting fluid. The wafers were then cleaned ultrasonically. Powdered materials were prepared by crushing the source material until it passed through a 40-mesh (420- $\mu$ m) sieve, then collecting the -40/+80-mesh (-420/+177- $\mu$ m) fraction. The powdered fraction was cleaned ultrasonically in water to remove electrostatically adhered fine particles. Specific surface areas of these powders were estimated to be 45.9 cm<sup>2</sup>/g for the Synroc powders and 66.7 cm<sup>2</sup>/g for the 76-68 glass powders. These estimates were obtained by assuming cubic geometry with a 300- $\mu$ m edge for all particles and a density of 4.35 g/cm<sup>3</sup> for Synroc-C and 3.00 g/cm<sup>3</sup> for 76-68 glass. Some preliminary leach testing comparing monoliths and powders at equal SA/V ratios based on the above estimated surface areas yielded similar results, which provided confidence in the surface area estimates.

The MCC-1 tests using monolithic test specimens were conducted at SA/V ratios of 0.1 cm<sup>-1</sup> (10 m<sup>-1</sup>) for periods of up to 28 days. These tests were conducted at 90°C and 150°C in silicate water<sup>(b)</sup> with a pH of 8.67 and in a brine<sup>(c)</sup> with a pH of 4.43. The MCC-3 tests were conducted for periods of up

---

(a) Nominal composition of Synroc-C was supplied with the 500-g sample that was shipped to PNL by W. J. Buykx of the Australian Atomic Energy Commission.

(b) 0.002 M NaHCO<sub>3</sub>, 0.001 M SiO<sub>2</sub>.

(c) 0.65 M KCl, 1.54 M NaCl, 1.22 M MgCl<sub>2</sub>.

TABLE 1. Compositions of U-Doped 76-68 Glass and Synroc-C

<u>Oxide</u>	<u>76-68 Glass, wt%</u>	<u>Synroc-C, wt%</u>
Ag <sub>2</sub> O	0.0	0.02
Al <sub>2</sub> O <sub>3</sub>	0.85	4.86
B <sub>2</sub> O <sub>3</sub>	8.55	0.0
BaO	0.62	5.34
CaO	2.11	9.99
CdO	0.0	0.02
CeO <sub>2</sub>	0.97	1.22
Cr <sub>2</sub> O <sub>3</sub>	0.45	0.083
Cs <sub>2</sub> O	0.77	0.83
Fe <sub>2</sub> O <sub>3</sub>	8.16	0.38
Gd <sub>2</sub> O <sub>3</sub>	0.0	0.37
La <sub>2</sub> O <sub>3</sub>	5.07	0.0
MoO <sub>3</sub>	1.99	1.31
Na <sub>2</sub> O	9.66	0.0
Nd <sub>2</sub> O <sub>3</sub>	1.61	1.55
NiO	0.22	0.031
P <sub>2</sub> O <sub>5</sub>	0.60	0.17
PdO	0.0	0.37
RuO <sub>2</sub>	0.0	0.75
Rh <sub>2</sub> O <sub>3</sub>	0.0	0.12
TeO <sub>2</sub>	0.0	0.19
SiO <sub>2</sub>	40.50	0.0
SrO	0.46	0.27
TiO <sub>2</sub>	2.60	64.2
UO <sub>2</sub>	4.16	0.49
Y <sub>2</sub> O <sub>3</sub>	0.0	0.16
ZnO	4.34	0.0
ZrO <sub>2</sub>	<u>1.88</u>	<u>7.37</u>
Total	95.57	100.09

to 90 days at SA/V ratios of  $4.6 \text{ cm}^{-1}$  for Synroc powders and  $6.7 \text{ cm}^{-1}$  for 76-68 glass powders with the same solutions and temperatures as the monolith specimens. In both types of tests, solution samples were collected after cooling to room temperature, pH values were measured, and the solutions were filtered through  $0.5\text{-}\mu\text{m}$  filters. Solutions from the MCC-3 powder tests were also filtered through  $1.8\text{-nm}$  filters. Solutions from the monolith tests were acidified before analysis, and those from the powder tests were both acidified and diluted before analysis. All solution analyses were done by inductively coupled plasma spectroscopy (ICP); uranium analyses were done by laser fluorescence spectroscopy.

Some additional tests were done with monolith samples to determine if sorption on container walls might result in unacceptable leachate composition changes. In Table 2, Mo, Cs, and U concentrations in both silicate water and brine solutions are compared for  $90^\circ\text{C}$  and  $150^\circ\text{C}$  monolith tests. In one case, leachates were directly sampled after cooling to room temperature. In the second case, the solid sample was removed after the experiment, then the leachate was acidified in the leach container, which was returned to the oven overnight at the experimental temperature. There did not appear to be a large composition effect due to sorption on container walls; therefore, subsequent leachates were directly sampled.

TABLE 2. Leachate Composition Changes Due to Sorption on Container Walls

Results from 90°C, 28-day, MCC-1 Tests

Material <sup>(a)</sup>	Preparation <sup>(b)</sup>	Leachate <sup>(c)</sup>	Mo, ppm	Cs, ppm	U, ppm
G	D	S	2.28	1.70	1.21
G	D	S	2.29	1.70	1.27
G	H	S	2.29	1.70	1.43
G	H	S	2.06	1.60	1.20
G	D	B	1.79	0.88	0.0
G	D	B	1.95	0.50	0.0
G	H	B	1.84	0.75	0.13
G	H	B	1.95	0.92	0.14
S	D	S	0.18	0.045	0.002
S	D	S	0.18	0.018	0.0
S	D	S	0.19	0.039	0.002
S	H	S	0.19	0.047	0.008
S	H	S	0.18	0.026	0.003
S	H	S	0.18	0.035	0.0

Results from 150°C, 14-day, MCC-2 Tests

G	D	S	5.52	1.56	1.56
G	D	S	9.24	6.20	1.78
G	H	S	5.54	5.50	1.62
G	H	S	9.33	4.90	1.66
S	D	S	0.25	0.066	0.0
S	D	S	0.25	0.075	0.0
S	H	S	0.40	0.072	0.001
S	H	S	0.28	0.066	0.002
S	D	B	0.37	0.0	0.0
S	D	B	0.41	0.0	0.17?
S	H	B	0.42	0.0	0.07
S	H	B	0.41	0.0	0.05

(a) G = 76-68 glass; S = Synroc-C.

(b) D = leachate sample taken directly after experiment; H = leachate acidified in original container and held overnight at experimental temperature.

(c) S = silicate water; B = brine.

## RESULTS AND DISCUSSION

The durability of Synroc-C in silicate water systems as compared with 76-68 glass can be considered in terms of the dissolution of Ba, Cs, Mo, and U. These elements can be detected in leachate solutions, usually with reasonable precision, and are common to both waste forms. The amounts of Cs and Mo in Synroc-C are about the same as in 76-68, but Ba is a major component of Synroc while present in only minor amounts in glass (Table 1). Ba is the major cation in the Hollandite phase ( $\text{BaAl}_2\text{Ti}_6\text{O}_{16}$ ) of Synroc, which also contains Cs in channel sites, while Mo is considered to partially substitute for Ti in the Perovskite phase ( $\text{CaTiO}_3$ ) (Ringwood and Kesson 1979). U is assumed to be predominantly bound in the Zirconolite phase ( $\text{CaZrTi}_2\text{O}_7$ ). These are the three major phases of Synroc (Ringwood and Kesson 1979).

Determining the dissolution rates of these four elements from the Synroc phases compared with their rates from glass, based on MCC-1-type tests and low SA/V temperature-dependent tests, provides an indication of the durability of Synroc compared with glasses such as 76-68. The high SA/V MCC-3-type tests are intended to determine if saturation concentrations are approached for these elements.

Leach test results from silicate water systems are emphasized in this section because they are more extensive than results from brine systems. However, selected results from tests in brine systems are also presented in this section. More detailed test results for monolith and powder specimens in both silicate water and brine systems are presented in the appendices.

### SILICATE WATER LEACH TEST RESULTS

In a relatively unbuffered low-ionic-strength solution, the change in initial and final pH values during leaching is an approximate measure of waste form reactivity, which includes alkali-hydrogen ion exchange along with hydrolysis and dissociation of dissolved species. The initial pH of silicate water (8.6) increased to less than 9.0 in MCC-1 tests with both Synroc and glass monoliths for up to 28 days. All pH measurements were made at room temperature, and no distinct trends were apparent from the monolith tests.

Measurements of pH for the high SA/V powder tests (MCC-3) at both 90°C and 150°C are shown in Figure 1. The maximum change in pH for all systems was from about 8.6 to 10.1; and, in most cases, replicate pH measurements were reproducible to less than a half a pH unit. In spite of these relatively small changes, some trends are apparent. In general, pH values increased with both time and temperature for both materials as the reaction progressed. This trend was expected for waste systems, especially glass systems (Grambow 1984; Shade and Strachan 1985). The increase in pH, relative to initial values, observed for the 76-68 glass was greater than for Synroc and is a reflection of the higher reactivity of glass. A positive slope is shown at 56 and 90 days in Figure 1 for 150°C Synroc pH values, but these values may also be considered constant within the uncertainty of measurement. A constant pH for these time periods would be consistent with results, discussed later, that suggest several elements released from Synroc may have achieved saturation.

Results from the MCC-1 tests at 90°C and 150°C are shown in Figures 2 through 5. Ba concentrations from monolith Synroc and glass specimens are given in Figure 2. These concentrations were not normalized because Ba is essentially an impurity in glass. Although the Ba concentrations were low, they do suggest a slight temperature dependence for Synroc. The source of Ba may be from the Hollandite phase or more likely from residual Ba in a less stable host.

Normalized concentrations of Cs, Mo, and U are given in Figures 3, 4, and 5. These data were normalized to the weight fraction of the element in the waste form. Both Cs and Mo release rates from glass and Synroc exhibited similar behavior. Based on the normalized concentrations of these elements from 90°C tests, release rates from glass were about an order of magnitude higher than those from Synroc. At 150°C, these same rates were more than an order of magnitude higher for glass than for Synroc. Synroc also exhibited less temperature dependence on leach rates than glass, which supports the suggestion that Cs and Mo are in structurally dissimilar sites for the two materials. Normalized U data from MCC-1 tests indicate that U release rates in glass were more than an order of magnitude higher than in Synroc (Figure 5). There was little temperature dependence of U release for both materials, but this may be

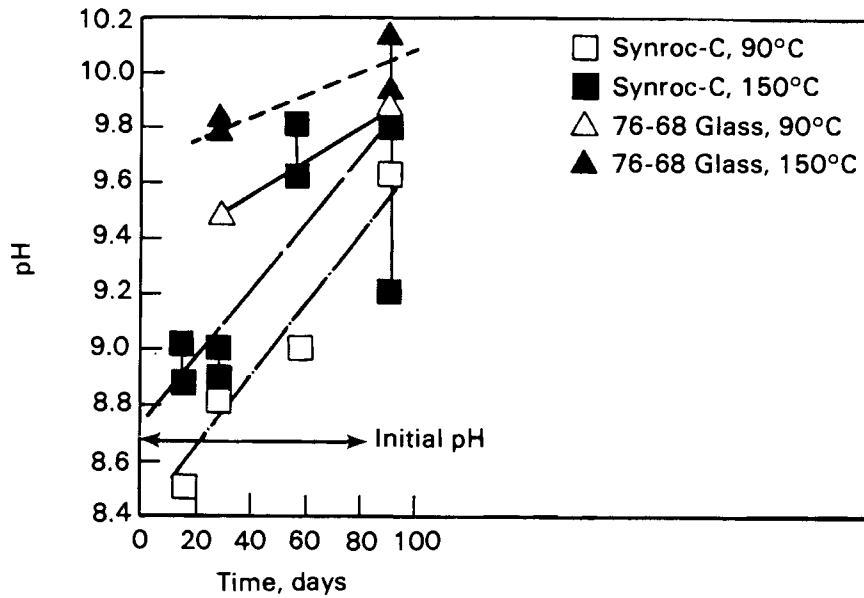


FIGURE 1. Final pH Values from Silicate Water Tests with Powders at 90°C and 150°C

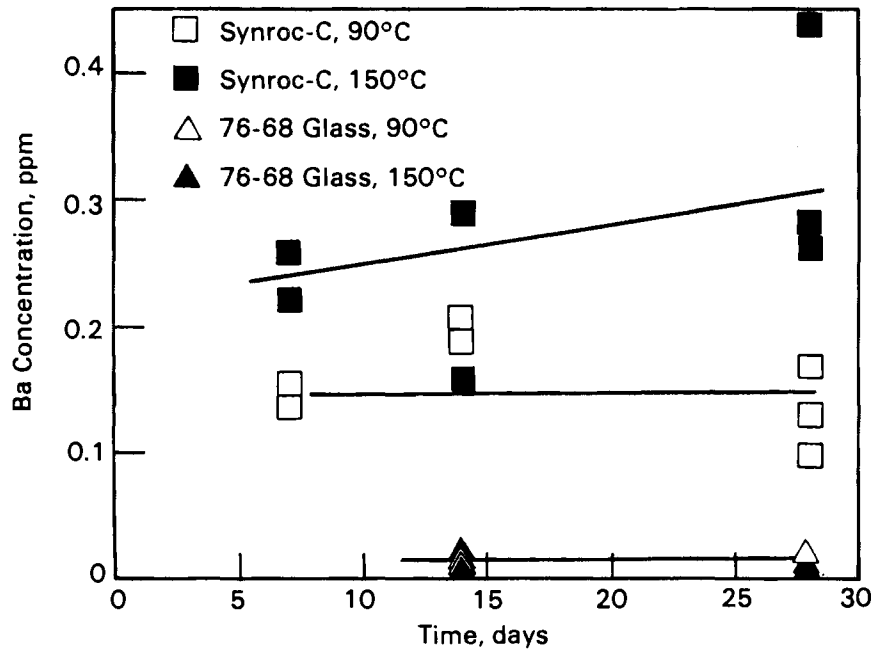


FIGURE 2. Ba Concentrations for Synroc-C and 76-68 Glass Monoliths in Silicate Water at 90°C and 150°C

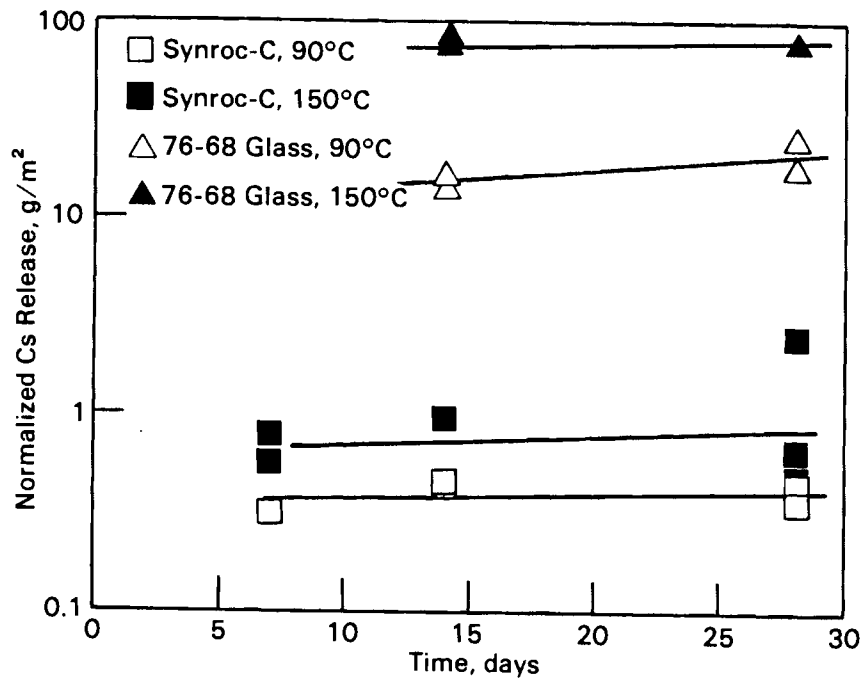


FIGURE 3. Normalized Cs Dissolution from Synroc-C and 76-68 Glass Monoliths in Silicate Water Tests at 90°C and 150°C

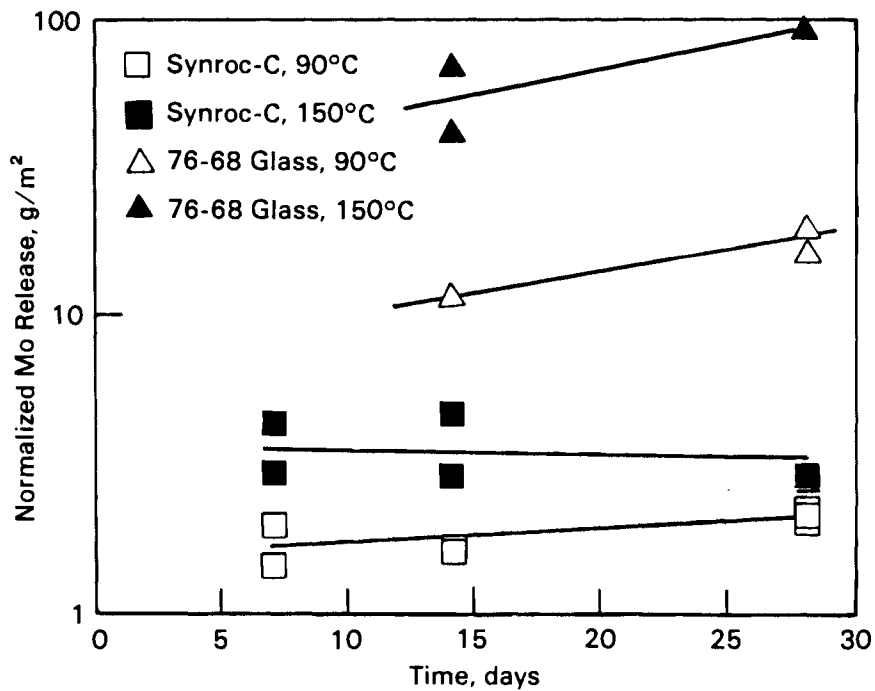


FIGURE 4. Normalized Mo Dissolution from Synroc-C and 76-68 Glass Monoliths in Silicate Water Tests at 90°C and 150°C

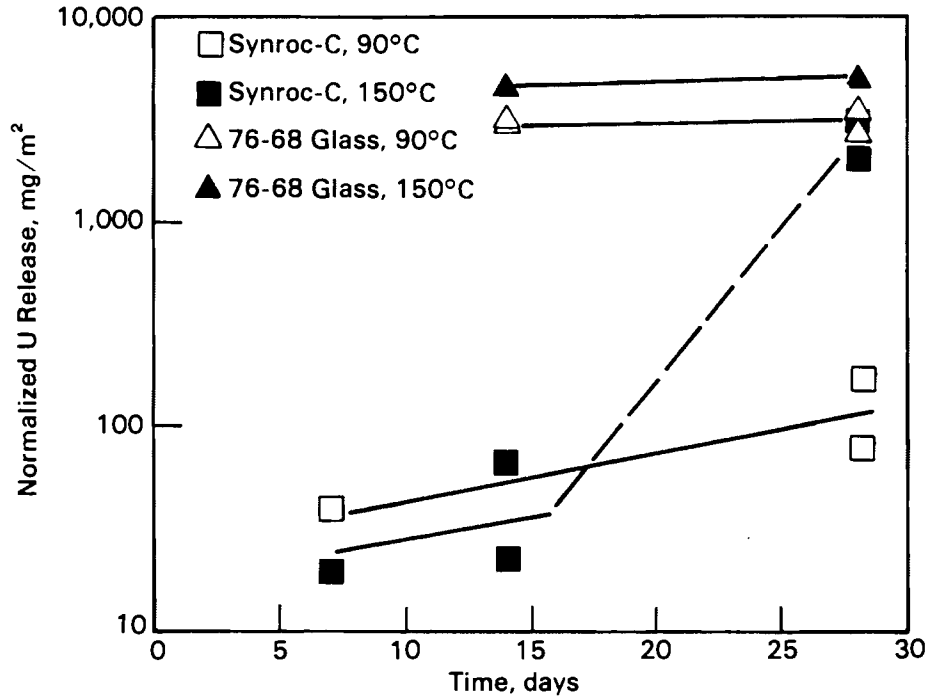


FIGURE 5. Normalized U Dissolution from Synroc-C and 76-68 Glass Monoliths in Silicate Water Tests at 90°C and 150°C

partly caused by some precipitation during sample cooling. The high U values at 28 days for the 150°C Synroc tests are uncertain because a replicate yielded low values. However, there seemed to be a slight increase in U release with time for the Synroc tests; but U release from glass may have become saturated at an early stage in the dissolution process. The U concentrations observed from the dissolution of 76-68 glass that correspond to the normalized release values in Figure 5 are between 1 and 2 ppm. Concentrations of about 2 ppm were also measured for short (28-day) time periods in high surface area powder tests (see Figure 8). Within this range, U concentrations were also measured in filtrates from other powder tests with 76-68 glass (Shade and Strachan 1986). Total U concentrations of about 2.4 ppm ( $10^{-5}$  mol/L) were measured at 25°C in solubility studies of schoepite ( $UO_3 \cdot 2H_2O$ ) between pH values of 9 to 10 (Krupka et al. 1985), which is in reasonable agreement with glass values considering the precision of U analyses. Thus, a possible limiting control of U concentrations in the early stages of dissolution may be a hydrated U(VI) phase.

Results from the high SA/V powder tests (MCC-3) at 90°C are shown in Figures 6 through 8. These data are presented in terms of concentration units

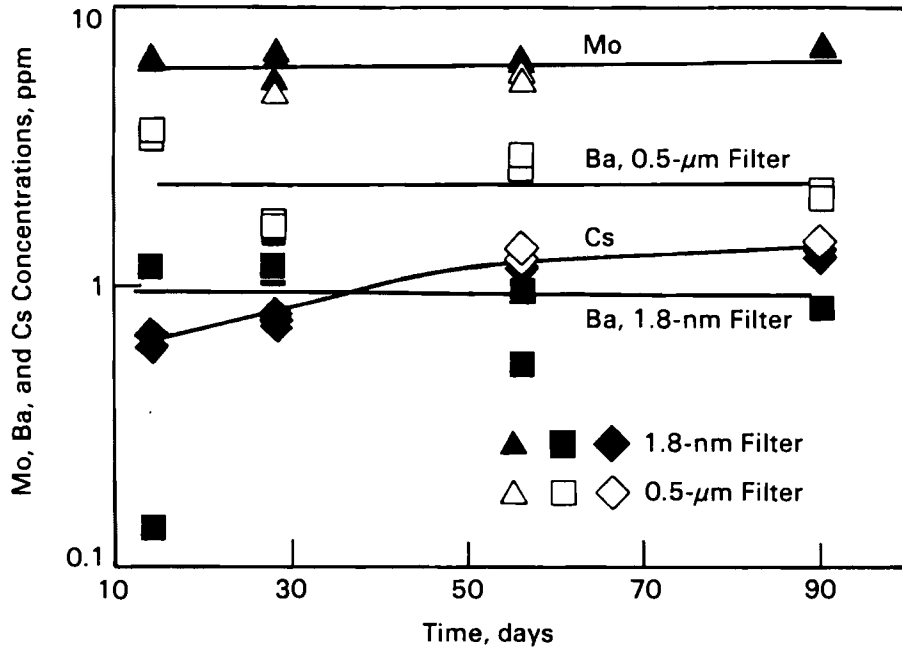


FIGURE 6. Ba, Cs, and Mo Concentrations in 0.5- $\mu\text{m}$  and 1.8-nm Filtrates of Silicate Water from Synroc-C Powder Tests at 90°C

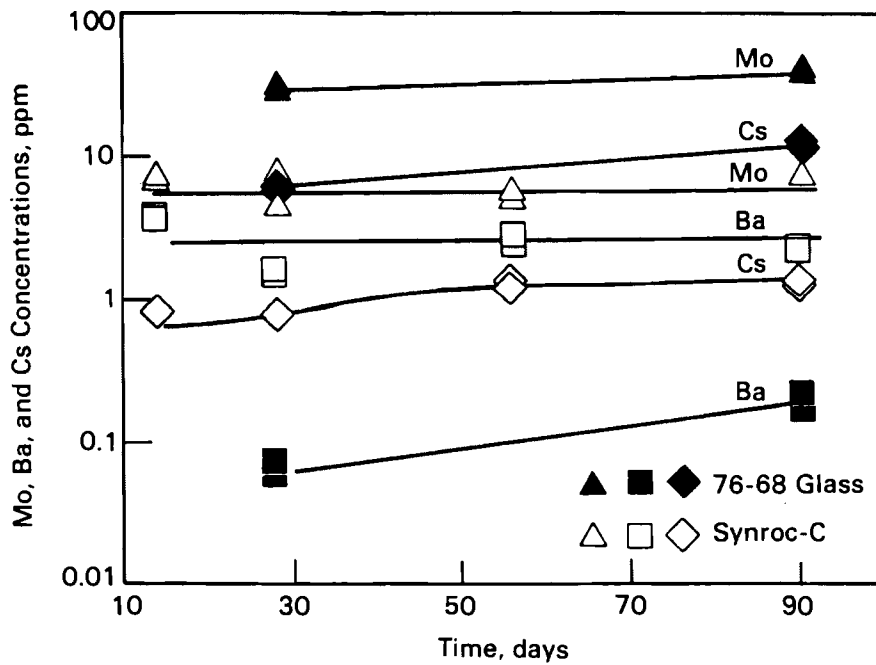


FIGURE 7. Ba, Cs, and Mo Concentrations for Synroc-C and 76-68 Glass Powders in 0.5- $\mu\text{m}$  Filtrates of Silicate Water at 90°C

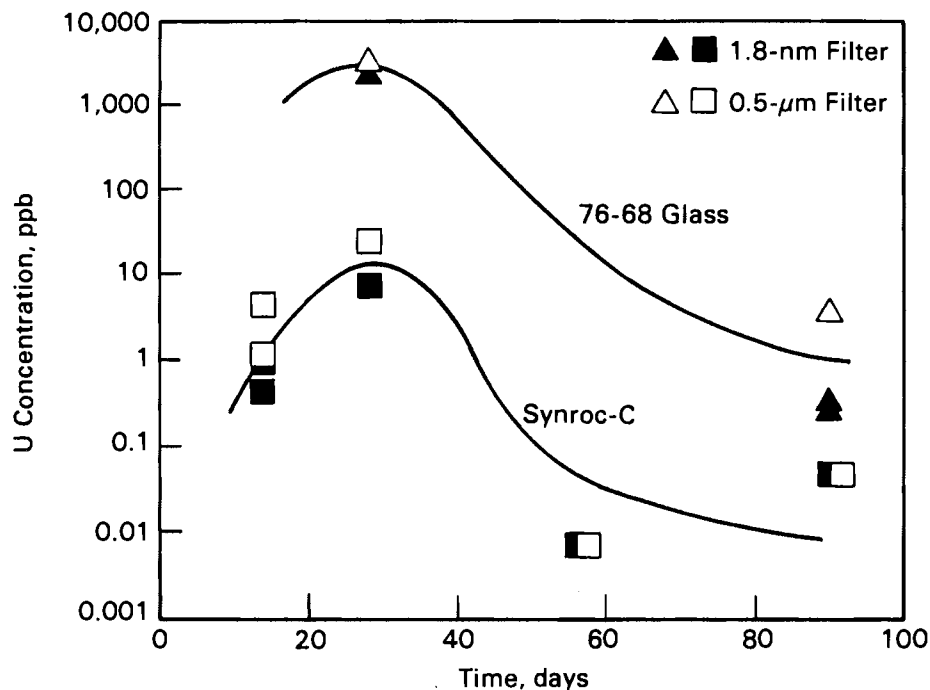


FIGURE 8. U Concentrations from 0.5-µm and 1.8-nm Filtrates of Synroc-C and 76-68 Powders in Silicate Water at 90°C

rather than normalized units because these tests measured saturation concentrations. For those who prefer other units, the SA/V was  $4.6 \text{ cm}^{-1}$  for the Synroc tests and  $6.7 \text{ cm}^{-1}$  for the glass tests.

The Mo, Ba, and Cs, concentrations in Synroc leachates after filtering through 0.5-µm filters and then 1.8-nm filters are shown in Figure 6. These data indicate that Cs and Mo concentrations did not change after filtration, suggesting that these elements occur as dissolved species rather than particulates or colloids. It also appears that saturation has been achieved for Mo and closely approached for Cs. Within the scatter of the data, Ba seems to have reached saturation; but part of the total Ba exists in particulate form as might be expected at the relatively high pH values in these systems.

The concentrations of the same elements from 0.5-µm filtrates are compared for Synroc and glass systems in Figure 7. As indicated in earlier results, Mo and Cs concentrations were about an order of magnitude higher in 76-68 systems than in Synroc. On the basis of only two time periods, Mo and Cs concentrations seemed to increase with time for glass but may have reached saturation

values for Synroc. Ba concentrations were lower in the glass than in Synroc; but Ba appears to have achieved saturation values in Synroc, which may suggest a steady-state condition with respect to Hollandite solubility or simply indicate removal of Ba from intergranular sites.

The U data from these tests are shown in Figure 8. Concentrations of U were up to two orders of magnitude higher in glass than in Synroc, which is consistent with the results obtained for monolith tests. Maximum concentrations for both materials were observed at 28 days, but these values decreased by about two orders of magnitude at 90 days. At the low U concentrations measured at 90 days, analytical precision is such that uncertainties in U values are about an order of magnitude. In view of this analytical uncertainty, the trend of U concentrations with time can be considered to eventually converge for both materials to a value lower than the maximum observed at 28 days. Controls on U concentrations can then be interpreted in terms of sequential formation of U solid phases. For example, if the high U values observed at short time periods are assumed to be controlled by the solubility of a hydrated U(VI) phase, then subsequent reaction of this phase with both alkali and silica (from either the initial liquid or the waste form) could result in the formation of an alkali uranium silicate such as sodium baltwoodite  $[\text{Na}_2(\text{UO}_2)_2(\text{SiO}_3)_2(\text{OH})_2 \cdot 5\text{H}_2\text{O}]$  or weeksite  $[\text{K}_2(\text{UO}_2)_2(\text{Si}_2\text{O}_5)_3 \cdot 4\text{H}_2\text{O}]$ . Baltwoodite has been observed in experimental studies of U-bearing silicate water-basalt systems at temperatures as low as 60°C (Kelmers et al. 1986).

The Cs and Mo concentrations from the high SA/V powder tests, the monolith tests, and the short-term (1-day) tests at 90°C and 150°C were combined in terms of SA/V x time as shown in Figures 9 through 12. The SA/V x time parameter provides an indication of concentrations that might be expected in flow tests if the surface area divided by flow rate can be considered to be a reasonable approximation for this parameter. At high SA/V x time values, saturation concentrations can be determined, which provide  $C_i$  values for the flux ratio (Zavoshy, Chambre, and Pigford 1985). Low SA/V x time values (such as  $\log \text{SA/V} \times \text{time} = -1.0$ ) provide an approximation to the forward dissolution rate ( $J_0$ ).

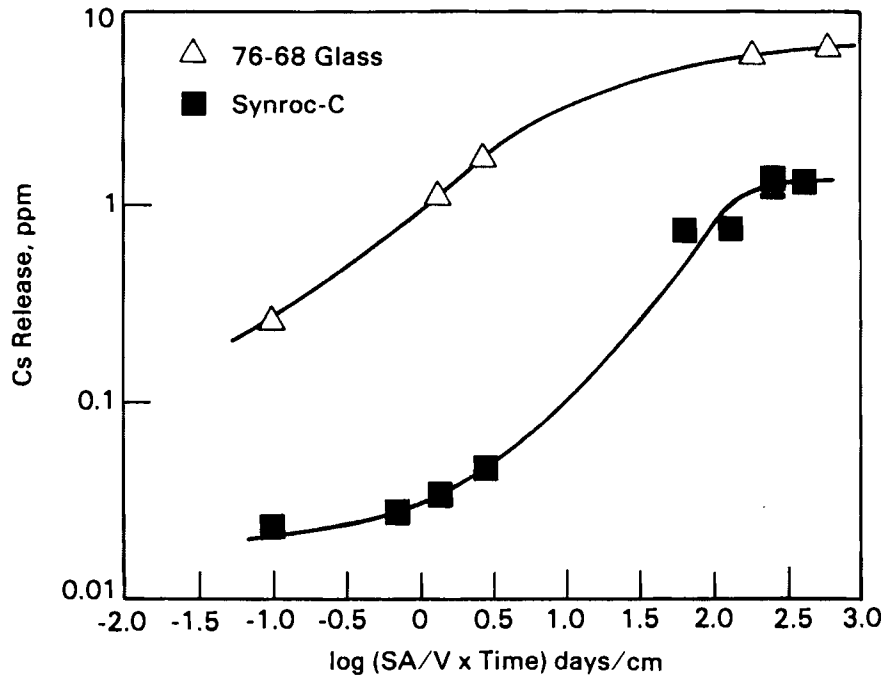


FIGURE 9. Cs Concentrations in 0.5- $\mu$ m Filtrates from Monolith and Powder Tests for Synroc-C and 76-68 Glass in Silicate Water at 90°C

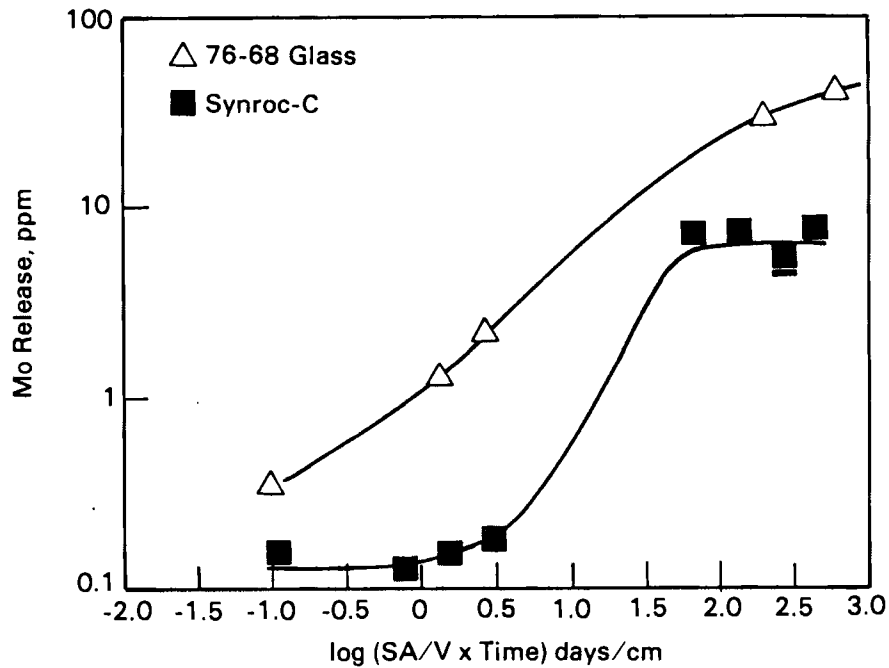


FIGURE 10. Mo Concentrations in 0.5- $\mu$ m Filtrates from Monolith and Powder Tests for Synroc-C and 76-68 Glass in Silicate Water at 90°C

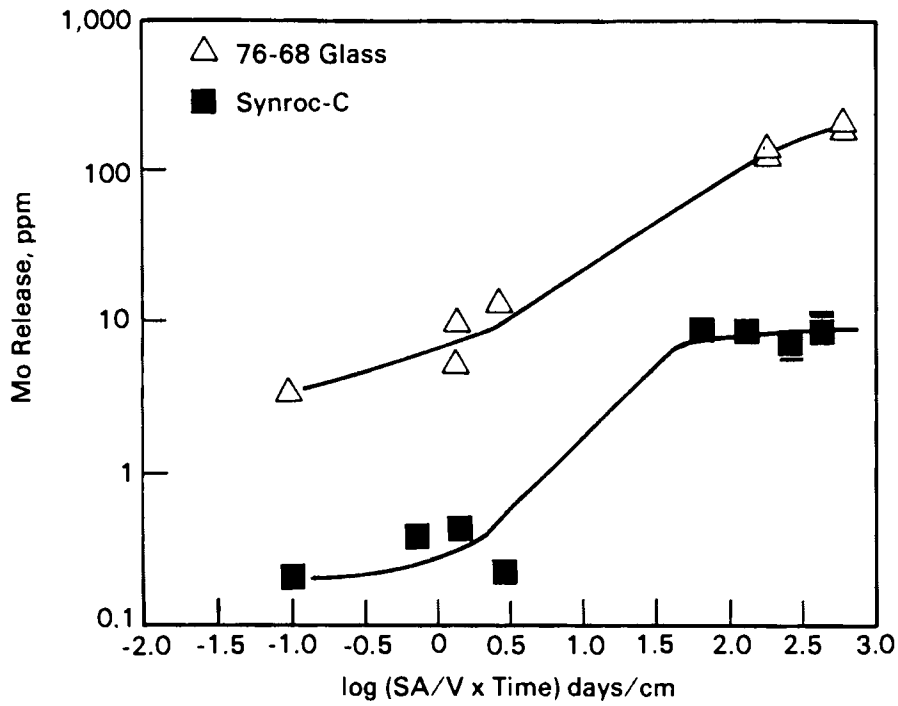


FIGURE 11. Mo Concentrations in 0.5- $\mu$ m Filtrates from Monolith and Powder Tests for Synroc-C and 76-68 Glass in Silicate Water at 150°C

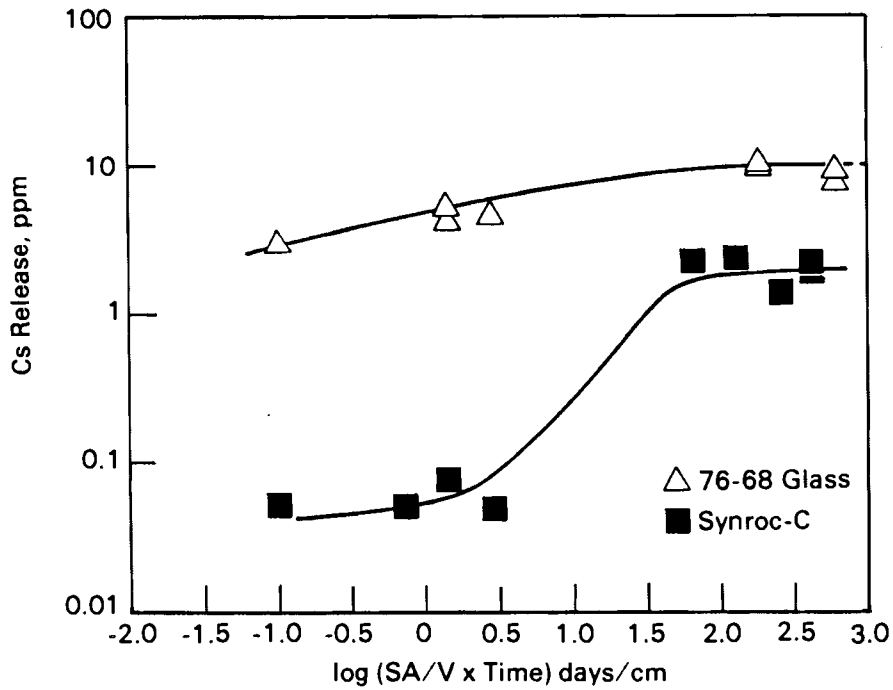


FIGURE 12. Cs Concentrations in 0.5- $\mu$ m Filtrates from Monolith and Powder Tests for Synroc-C and 76-68 Glass in Silicate Water at 150°C

Cs concentrations for Synroc and 76-68 glass at 90°C (Figure 9) indicated an approach to saturation for both waste forms, although the Cs release from glass was almost an order of magnitude higher than from Synroc. If these saturation values can be considered as crude approximations of solubility values for Cs-bearing solids, the concentration differences support the fact that Cs in glass is chemically bound in different types of structural sites than in Synroc. This supposition is consistent with the assertion that Cs in Synroc is located in channels in the Hollandite phase (Ringwood and Kesson 1979) but is less localized in glass. It has been reported (Levins 1985) that Cs release from Synroc increases linearly with SA/V, with a slope near unity. At the SA/V ratios investigated (about 4.0 to 250 cm<sup>-1</sup>), very little time dependence was observed at a given SA/V. The highest SA/V value considered in the present work was 6.7 cm<sup>-1</sup> (Figure 9); and after 56 days, Cs appeared to approach saturation at values near 1.0 ppm, which is in agreement with Levins (1985). The rapid increase in Cs with SA/V ratios of Synroc described in Levins (1985) may be the result of increasing exposure of Cs-bearing channels in Hollandite as surface areas increase rather than by formation of a reaction product whose solubility controls Cs concentration. Another possibility is that the Cs released is from intergranular sites rather than from crystalline sites, so only residual Cs that is not structurally bound in crystals is dissolved. This type of mechanism has been suggested by Cooper et al. (1986) on the basis of high-resolution electron microscope examination of Synroc-C. Thus, as surface area increases, more intergranular sites are exposed. In the case of residual dissolution of intergranular Cs, a pulsed release would probably be expected rather than a continual release; thus, little time dependence would be observed.

Dissolution of Mo as a function of SA/V x time at 90°C is compared for 76-68 and Synroc in Figure 10. Mo concentrations were about an order of magnitude higher than Cs concentrations at this temperature, and Mo concentrations from glass were higher than those from Synroc by about the same amount. Mo saturation appears to have been attained for Synroc but not for glass, which may be the result of intergranular release of Mo as suggested for Cs.

The forward-direction leach rate and saturation concentrations can be obtained from the data that are compiled in figures such as Figures 9 and 10. These data can be used to calculate transport-related parameters such as the flux ratio (Zavoshy, Chambre, and Pigford 1985), which was described previously. For example, the Cs flux ratio is calculated from the data in Figure 9 for Synroc and 76-68 glass assuming a canister radius ( $r_0$ ) of 0.44 m and a porosity ( $e$ ) of 0.01. At a value of -1.0 day/cm for log SA/V x time in Figure 9, the Cs concentrations are 0.03 ppm for Synroc and 0.4 ppm for 76-68 glass. The SA/V ratio for both materials was  $10 \text{ m}^{-1}$  and the leach test was conducted for 1 day, so the forward leach rate ( $j_0$ ) was  $0.003 \text{ g/m}^2\text{-day}$  for Synroc and  $0.04 \text{ g/m}^2\text{-day}$  for glass. The saturation values ( $C_s$ ) can be obtained in the region where log SA/V x time is 2.5 day/cm and is about 1.0 ppm ( $\text{g/m}^3$ ) for Synroc and about 8 ppm ( $\text{g/m}^3$ ) for glass. Using a diffusion coefficient ( $D$ ) for Cs of  $3.4 \times 10^{-4} \text{ m}^2/\text{day}$  and substituting these values into the flux ratio equation yields a Synroc flux ratio of  $3.9 \times 10^2$  and a glass flux ratio of  $6.5 \times 10^2$ . Thus, under these conditions, both glass and Synroc exhibit flux ratios much greater than unity so that Cs removal from both waste forms would probably be transport controlled by diffusive/convective processes.

Mo and Cs values at  $150^\circ\text{C}$  are shown in Figures 11 and 12; the trends are similar to those at  $90^\circ\text{C}$ . The glass consistently yielded a greater temperature dependence than Synroc. At low SA/V x time values, the data in Figure 11 suggest that Cs was nearly saturated for glass systems at  $150^\circ\text{C}$ . Mo continued to dissolve from the glass at  $150^\circ\text{C}$  at high SA/V x time values and showed no indication of saturation.

The estimated forward leach rates for Cs and Mo from Synroc and 76-68 glass in the temperature range from 90 to  $250^\circ\text{C}$  are shown in Figure 13. These elements were selected because they do not tend to form precipitates or colloidal species during cooling of dilute solutions. Cs and Mo determinations were made from tests in which the SA/V for both materials was  $0.1 \text{ cm}^{-1}$  using the -40/+80 mesh size. The tests were conducted in deionized water for 24 h; thus, the SA/V x time value is 0.1 day/cm. These parameters were selected to obtain measurable amounts of Cs and Mo at the lowest SA/V x time value possible and to avoid the occurrence of back reactions or precipitation. Another approach was

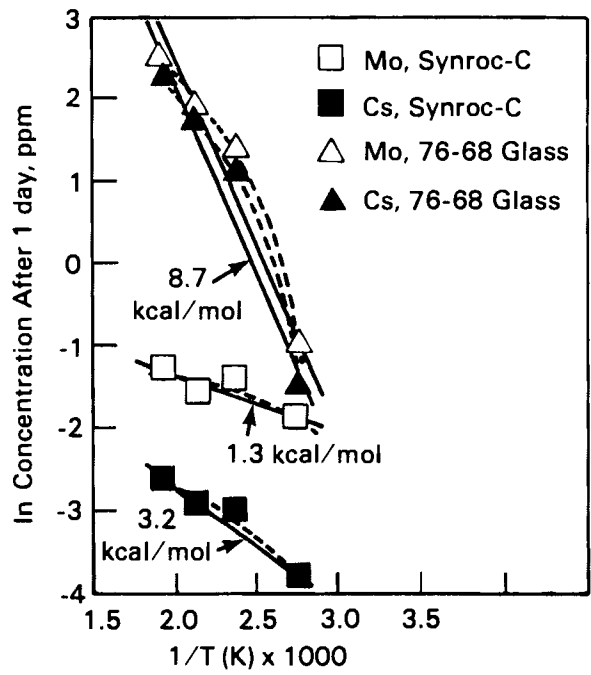


FIGURE 13. Temperature Dependence of Mo and Cs Forward Dissolution Rates Between 90°C and 250°C for Synroc-C and 76-68 Glass in Silicate Water

attempted in which the leach times were decreased in proportion to the temperature differences so that the shortest leach times occurred at the highest temperatures. Results from this approach were not satisfactory because Cs and Mo concentrations were near or below detection limits.

Measurements of glass leaching rates at different temperatures resulted in pH changes that increased, relative to initial pH values, at higher temperatures. The initial pH value for deionized water was about 6.0, and final values after 1 day were 8.6 at 90°C and 9.4 at 200°C. This increase occurred in part because more of the hydrolyzable elements, such as Na, were leached from the glass at higher temperatures than at lower temperatures. At higher temperatures, a greater fraction of the initial deionized water was in the vapor phase; thus, less liquid water was in contact with the waste form. Dissociation constants and water ionization constants are temperature dependent, but Cs and Mo values were determined at ambient temperature. These temperature effects are probably the dominant cause of the curvature exhibited by the data in Figure 13. The curvature was more pronounced in glass than in Synroc

because more material was in solution and participated in hydrolysis reactions. These data are considered to represent an approximation of the forward leach rate, and the curvature is not considered to be indicative of a change in leaching mechanism with temperature. Samples obtained at temperature would probably provide better results, but equipment to do this was not available.

Activation energies were calculated from the Cs and Mo data in Figure 13 using slopes for the solid straight lines, which are considered to represent the actual data trends. Cs and Mo release rates from glass systems showed a nearly identical trend, which suggests they are released from structurally similar sites in glass. The activation energy of about 8.7 kcal/mol based on these elements is consistent with dissolution rates controlled by reactions at the glass surface (Lasaga and Kirkpatrick 1981). The low activation energies for Mo and Cs dissolution rates in Synroc of 1.3 and 3.2 kcal/mol, respectively, as well as the low concentrations suggest that these elements may be released from intergranular or other sites in which they are not strongly bonded rather than from locations in crystalline phases. That is, the source of these elements might be from residual amorphous material remaining after waste form fabrication. The difference in activation energies also suggests that Cs and Mo are associated with sites that are nearly, but not exactly, chemically identical. The low activation energies are also consistent with the observation of unit increase of Cs dissolution with SA/V if it is assumed that increased amounts of interstitial amorphous material are exposed as the Synroc surface area increases and that apparent Cs saturation is controlled by the amount of interstitial material dissolved.

#### BRINE LEACH TEST RESULTS

A relatively small number of tests were conducted to investigate the dissolution behavior of Synroc in brines. Both monolith and powder tests were conducted, but fewer sampling periods were used than in the silicate water tests. A summary of the results for Cs, Mo, Ca, Ba, and U is given in Tables 3 and 4. Additional brine test results are given in Appendices B and D. In these brine tests, the final pH values did not change very much from the

TABLE 3. MCC-1 and MCC-2 Brine Leach Data

Conditions	Time, days	Concentration, ppm				U Concentration, ppb
		Cs	Mo	Ca	Ba	
Synroc-C, 90°C	14	0.0	0.32	0.44	0.50	0.0
	28	0.0	0.31	0.90	0.61	0.0
	28	0.0	0.31	0.92	0.59	0.0
76-68 Glass, 90°C	28	0.75	1.80	2.5	0.96	130
	28	0.92	1.95	2.5	0.97	140
Synroc-C, 150°C	14	0.0	0.37	0.67	0.82	70
	14	0.0	0.41	0.71	0.97	50
	28	0.0	0.54	0.91	1.04	0
76-68 Glass, 150°C	28	4.0	8.4	11.5	4.08	2000

TABLE 4. MCC-3 Brine Leach Data

Conditions	Time, days	Concentration, ppm				U Concentration, ppb
		Cs	Mo	Ca	Ba	
Synroc-C, 90°C	28	0.73	9.54	1.16	7.27	0.03
	28	0.73	8.95	1.15	7.48	0.03
	90	1.50	7.87	4.04	6.38	0.05
	90	1.50	7.80	3.99	6.28	0.05
76-68 Glass, 90°C	28	43.1	42.9	62.5	22.4	0.03
	28	43.9	46.7	60.4	21.8	0.03
	28	43.3	46.8	62.6	22.5	0.03
Synroc-C, 150°C	28	1.4	12.0	4.75	16.2	0.03
	28	1.5	12.2	4.85	13.5	0.03
	90	1.5	10.8	10.6	13.9	0.05
	90	1.5	10.7	9.04	14.7	0.05
76-68 Glass, 150°C	28	117.0	10.2	153.5	55.4	0.03
	28	115.0	11.0	155.0	56.4	0.04
	28	122.0	10.5	149.3	53.7	0.03

initial values, at least within the precision of measurement (about one pH unit). Ca concentrations are listed in Tables 3 and 4 because they are readily measurable in brine tests but are generally low in silicate water tests. It is probable that Mg reactions with waste forms, such as the formation of Mg silicates in glass systems, led to Ca dissolution.

Concentrations of elements dissolved from Synroc and glass monoliths at 90°C and 150°C are listed in Table 3. Detection limits are higher for many elements in brine systems than in silicate water, but the relative dissolution behavior of the two materials can be determined. In general, dissolution from glass was higher than from Synroc, usually by about an order of magnitude. It is presumed that the increased dissolution of Ca in brine systems compared with silicate water is the result of Mg reactions with the waste forms.

Concentrations of elements from powder tests are given in Table 4. The same general dissolution trend as observed for monoliths was apparent, with glass exhibiting higher dissolution rates than Synroc. The U values for glass are questionable and may reflect analytical problems. The high values for Ba dissolved from glass powders is somewhat surprising because it is inconsistent with other results. Consequently, these Ba values may also be questionable. In perspective, however, results from both the monolith and powder tests indicate that the dissolution behavior of Synroc relative to glass in brine systems is similar to that observed in silicate water systems.

## REFERENCES

- Berner, R. A. 1978. "Rate Control of Mineral Dissolution Under Earth Surface Conditions." Am. J. Sci. 278:1235-1252.
- Bunnell, L. R., G. D. Maupin, and K. H. Oma. 1986. "High-Temperature Glasses for Nuclear Waste Isolation." PNL-SA-13606, presented at the American Ceramic Society Annual Meeting, Nuclear Waste Management Symposium, April 27-May 1, 1986, Chicago, Illinois.
- Casey, L. A., ed. 1978. "High-Level Radioactive Solid Waste Forms." In Proceedings of a U.S. Nuclear Regulatory Commission Conference, Denver, Colorado, NUREG/CP-0005.
- Chambre, P. L., S. J. Zavoshy, and T. H. Pigford. 1982. "Solubility-Limited Fractional Dissolution Rate of Vitrified Waste in Groundwater." Trans. Am. Nucl. Soc. 43:111.
- Chikalla, T. D., and J. E. Mendel, eds. 1979. "Ceramics in Nuclear Waste Management." Presented at the American Ceramic Society Symposium, Cincinnati, Ohio, CONF-790420.
- Cooper, J. A., et al. 1986. "Intergranular Films and Pore Surfaces in Synroc C: Structure, Composition, and Dissolution Characteristics." J. Am. Ceram. Soc. 69:347-352.
- Grambow, B. 1984. "Geochemical Modeling of the Reaction Between Glass and Aqueous Solution." In Advances in Ceramics, Vol. 8, Nuclear Waste Management, Wicks and Ross, eds., pp. 478-481, American Ceramic Society.
- Hayward, P. J., J. C. Tait, A. A. Carmichael, and J. P. M. Ross. 1986. "Source Term for Radionuclide Release from Sphere Glass-Ceramics." Presented at the American Ceramic Society Annual Meeting, Nuclear Waste Management Symposium, April 27-May 1, 1986, Chicago, Illinois.
- Kelmers, A. D., W. D. Arnold, J. G. Blencoe, R. E. Meyer, G. K. Jacobs, and S. K. Whatley. 1986. Progress in Evaluation of Radionuclide Geochemical Information Developed by DOE High-Level Nuclear Waste Repository Site Projects. NUREG/CR-4236, ORNL/TM-9614, Vol. 3, Oak Ridge National Laboratory, Oak Ridge, Tennessee.
- Krupka, K. M., D. Rai, R. W. Fulton, and R. G. Strickert. 1985. "Solubility Data for U(VI) Hydroxide and Np(IV) Hydrrous Oxide: Application of MCC-3 Methodology." Materials Research Society Symposium Proceedings, V. 44, Scientific Basis for Nuclear Waste Management, VIII, C. M. Jantzen et al., eds., pp. 753-760.
- Lasaga, A. C., and R. J. Kirkpatrick. 1981. "Kinetics of Geochemical Processes." Rev. in Mineralogy, Vol. 8, Mineral. Soc. Am., Washington, D.C.

- Levins, D. M. 1985. Performance of Synroc Under Conditions Relevant to Repository Disposal. Australian Atomic Energy Commission, IAEA report (presented in Japan).
- Materials Characterization Center. 1981. "MCC-1P Low Temperature Static Leach Test Method." In Nuclear Waste Materials Handbook, DOE/TIC-11400, National Technical Information Center, Springfield, Virginia.
- Materials Characterization Center. 1984. MCC-3 Agitated Powder Leach Test. PNL-3990, Pacific Northwest Laboratory, Richland, Washington (test method submitted to Nuclear Waste Materials Handbook).
- McCarthy, G. J., and M. T. Davidson. 1975. "Ceramic Nuclear Waste Forms - I. Crystal Chemistry and Phase Formation." Am. Ceram. Soc. Bull. 54:782-786.
- Mellinger, G. B., and J. L. Daniel. 1984. Approved Reference and Testing Materials for Use in Nuclear Waste Management Research and Development Programs. PNL-4955-2, Pacific Northwest Laboratory, Richland, Washington.
- Ringwood, A. E. 1978. Safe Disposal of High-Level Nuclear Reactor Wastes: A New Strategy. Australian National University Press, Canberra.
- Ringwood, A. E., and S. E. Kesson. 1979. "Immobilization of High-Level Waste in Synroc Titanate Ceramic." In Ceramics in Nuclear Waste Management, T. D. Chikalla and J. E. Mendel, eds., CONF-790420, pp. 174-182.
- Shade, J. W. 1981. "Comparison of Glass and Ceramic Leaching Behavior by Natural Analogs." Nucl. and Chem. Waste Mgmt. 2:219-228.
- Shade J. W., and D. M. Strachan. 1985. "Effect of High Surface Area to Solution Volume Ratios on Waste Glass Leaching." PNL-SA-13679, submitted to American Ceramic Society.
- Zavoshy, S. J., P. L. Chambre, and T. H. Pigford. 1985. "Mass Transfer in a Geologic Environment." Materials Research Society Symposium Proceedings, Vol. 44, Scientific Basis for Nuclear Waste Management, VIII, C. M. Jantzen et al., eds., pp. 311-322.

APPENDIX A

LEACH TEST RESULTS FROM MCC-1 AND MCC-2 TESTS ON  
SYNROC-C AND 76-68 GLASS IN SILICATE WATERS



TABLE A.1. MCC-1, Monolith, 90°C, Silicate Water<sup>(a)</sup>

	Material						
	Synroc-C	Synroc-C	U76-78	Synroc-C	Synroc-C	U76-68	U76-68
Size, cm	4.16	3.97	4.11	4.17	4.34	4.06	4.04
Fluid	Si H <sub>2</sub> O						
Volume, mL	41.6 <sup>2</sup>	39.7 <sup>2</sup>	41.1 <sup>2</sup>	41.7 <sup>2</sup>	43.4 <sup>2</sup>	40.6 <sup>2</sup>	40.4 <sup>2</sup>
Initial pH	8.67	8.67	8.67	8.67	8.67	8.67	8.67
Final pH	8.96	8.82	8.94	8.70	8.85	8.92	8.86
Time, days	7	14	14	28	28	28	28
Al	0.0151	0.0203	0.1563	2.1458	0.0316	0.1866	2.1840
B	0.0313	0.0254	2.7863	0.0332	0.0276	4.4608	4.3172
Ba	0.1510	0.2056	0.0112	0.0948	0.1276	0.0092	0.0208
Ca	0.0317	0.0559	0.2941	0.0744	0.0676	0.2774	0.3046
Cd	0.0007	0.0048	0.0005	0.0008	0.0032	0.0006	0.0150
Ce	0.0	0.0	0.0	0.0304	0.0912	0.0	0.1214
Cr	0.0053	0.0064	0.0030	0.0016	0.0066	0.0134	0.0200
Fe	0.0789	0.0350	0.0659	0.0848	0.0794	0.1364	0.2040
Mo	0.1330	0.1476	1.3393	0.1906	0.1808	2.2948	2.0596
Nd	0.0	0.0	0.0	0.0102	0.0196	0.0306	0.0510
P	0.0737	0.1537	0.1520	0.1222	0.0	0.2036	0.4936
Si	21.945	22.053	34.116	21.552	22.216	40.732	40.012
Ti	0.0044	0.0040	0.0018	0.0292	0.0066	0.0028	0.0122
Zn	0.0050	0.0077	0.0717	0.0144	0.0100	0.2042	0.1838
Zr	0.0020	0.0	0.0099	0.0372	0.0342	0.0916	0.0326
Cs	0.0270	0.0340	1.1	0.0470	0.0260	1.3	1.6
U(H), ppb <sup>(b)</sup>				8.5	3.3	1430.0	1200.0
U(R), ppb	1.7	0.0	1070.0	7.5	3.6400	1240.0	1130.0
K	0.1211	0.0617	0.2004	0.0	0.1270	0.2540	0.3386
Mg	0.0295	0.0230	0.0288	0.0	0.0584	0.0584	0.0972
Na	46.062	45.693	54.97	45.888	46.162	61.434	60.324

(a) Results are reported in ppm unless otherwise noted.

(b) (H) and (R) represent results from two different analysts.

TABLE A.2. MCC-2, Monolith, 150°C, Silicate Water<sup>(a)</sup>

	Material						
	Synroc-C	Synroc-C	Synroc-C	U76-68	Synroc-C	Synroc-C	U76-68
Size, cm	1.47	1.5	1.47	1.5	1.53	1.47	1.49
Fluid	Si H <sub>2</sub> O						
Volume, mL	14.7 <sup>2</sup>	15	14.7 <sup>2</sup>	15	15.3 <sup>2</sup>	14.7 <sup>2</sup>	14.9 <sup>2</sup>
Initial pH	8.67	8.67	8.67	8.67	8.67	8.67	8.67
Final pH	8.81	8.68	8.96	8.87	9.34	9.64	9.25
Time, days	7	14	14	14	28	28	28
Al	0.0347	0.0530	1.2168	4.6964	0.0422	0.0149	0.7278
B	0.0475	0.1534	0.0864	11.217	0.0390	0.0338	24.574
Ba	0.2223	0.2882	0.1808	0.0196	0.2622	0.4422	0.0083
Ca	0.4184	0.0676	0.1556	0.1556	0.6041	0.1877	0.2347
Cd	0.0012	0.0000	0.0	0.0	0.0	0.0	0.0
Ce	0.0	0.0308	0.0526	0.0	0.0149	0.0150	0.1192
Cr	0.0025	0.0016	0.0050	0.0436	0.0107	0.0061	0.1107
Fe	0.0422	0.0378	0.0626	0.3936	0.4046	0.0464	0.2510
Mo	0.3782	0.4010	0.2806	5.5400	0.2348	0.2532	12.850
Nd	0.0	0.0	0.0	0.0	0.0048	0.0	0.0599
P	0.1605	0.0	0.0	0.0490	0.1294	0.0431	0.6809
Si	22.254	22.910	22.576	96.25	22.925	24.254	119.5
Ti	0.0064	0.0170	0.0330	0.0198	0.0275	0.0243	0.0104
Zn	0.0566	0.0136	0.0072	0.5746	0.0453	0.0277	0.5974
Zr	0.0399	0.0184	0.0246	0.0462	0.1089	0.1614	0.0503
Cs	0.0460	0.0720	0.0660	5.5	0.0480	0.19	5.4
U(R), ppb	1.7	1.9	100.0	1370			
U(H), ppb	0.0	1.0	2.0	1620.0	140.0	90.0	1860.0
K	0.0462	5.3694	0.5584	1.1168	0.0214	0.0642	2.0334
Mg	0.0518	6.0750	0.3944	0.5918	0.0378	0.0095	1.2665
Na	45.934	53.664	46.236	82.838	47.203	49.499	121.11

(a) Results are reported in ppm unless otherwise noted.

APPENDIX B

LEACH TEST RESULTS FROM MCC-1 AND MCC-2 TESTS ON  
SYNROC-C AND 76-68 GLASS IN BRINE



TABLE B.1. MCC-1, Monolith, 90°C, Brine<sup>(a)</sup>

	Material			
	Synroc-C	Synroc-C	Synroc-C	U76-68
Size, cm	4.05	4.01	3.99	4.04
Fluid	Brine	Brine	Brine	Brine
Volume, mL	40.5	40.1	39.9	40.4
Initial pH	4.43	4.43	4.43	4.43
Final pH	6.38	3.72	3.59	4.88
Time, days	14	28	28	28
Al	0.0	0.0	0.0	0.0
B	0.134	0.134	0.104	3.683
Ba	0.537	0.564	0.564	0.968
Ca	0.353	0.794	0.424	2.454
Cd	0.012	0.0	0.012	0.048
Ce	0.509	0.680	0.512	0.337
Cr	0.144	0.153	0.099	0.135
Fe	0.156	0.192	0.240	0.162
Mo	0.292	0.252	0.385	1.949
Nd	0.453	0.571	0.344	0.521
P	0.000	0.0	0.0	0.0
Si	0.615	0.977	0.688	17.225
Ti	0.031	0.036	0.031	0.010
Zn	0.0	0.0	0.0	4.630
Zr	0.170	0.179	0.098	0.053
Cs	0.0	0.0	0.0	0.920
U(R), ppb	0.0	0.0	0.0	119.0
U(H), ppb	0.0	0.0	0.0	140.0

(a) Results are reported in ppm unless otherwise noted.

TABLE B.2. MCC-2, Monolith, 150°C, Brine<sup>(a)</sup>

	Material			
	Synroc-C	Synroc-C	Synroc-C	U76-68
Size, cm	1.51	1.48	1.42	1.45
Fluid	Brine	Brine	Brine	Brine
Volume, mL	15.1	14.8	14.2	14.5
Initial pH	4.43	4.43	4.43	4.43
Final pH	3.7	3.8	3.77	3.99
Time, days	14	14	28	28
Al	0.0	0.0	0.0	0.029
B	0.149	0.149	0.217	18.331
Ba	0.779	0.983	0.679	4.007
Ca	0.847	1.306	0.980	11.047
Cd	0.006	0.018	0.0	0.253
Ce	0.854	0.339	0.178	0.349
Cr	0.153	0.135	0.159	0.225
Fe	0.222	0.288	0.398	0.243
Mo	0.424	0.411	0.412	8.525
Nd	0.575	0.340	0.119	0.593
P	0.0	0.170	1.333	1.049
Si	0.832	1.194	1.067	81.522
Ti	0.057	0.046	0.058	0.037
Zn	0.0	0.0	0.0	23.901
Zr	0.554	0.644	0.589	0.844
Cs	0.0	0.0	0.0	4.0
U(R), ppb				
U(H), ppb	70.0	50.0	0.0	2000.0

(a) Results are reported in ppm unless otherwise noted.

APPENDIX C

LEACH TEST RESULTS FROM MCC-3 TESTS ON SYNROC-C  
AND 76-68 GLASS IN SILICATE WATER



TABLE C.1. MCC-3, Powder, 90°C, Silicate Water<sup>(a)</sup>

	Material								
	Synroc-C	Synroc-C	Synroc-C	Synroc-C	Synroc-C	Synroc-C	Synroc-C	Synroc-C	U76-68
Size	4080 Mesh <sup>(b)</sup>	4080 Mesh							
Fluid	Si H <sub>2</sub> O	Si H <sub>2</sub> O	Si H <sub>2</sub> O	Si H <sub>2</sub> O	Si H <sub>2</sub> O	Si H <sub>2</sub> O	Si H <sub>2</sub> O	Si H <sub>2</sub> O	Si H <sub>2</sub> O
Volume, mL	40	40	40	40	40	40	40	40	40
Initial pH	8.67	8.67	8.67	8.67	8.67	8.67	8.76	8.67	8.67
Final pH	8.52	8.52	8.52	8.52	8.82	8.82	8.82	8.82	9.5
Time, days	14	14	14	14	28	28	28	28	28
Al	0.1892	0.1010	0.1552	0.0982	0.1713	0.1313	0.1323	0.1439	0.2797
B	0.4460	0.0028	0.0056	0.0084	0.0478	0.5086	0.0401	0.2003	62.9670
Ba	3.3942	1.1146	3.4968	0.1384	1.5608	1.5087	1.6731	1.0713	0.0562
Ca	0.2300	0.2130	0.3212	0.3010	0.2500	0.2411	0.2978	0.3173	0.6293
Cd	0.0	0.0	0.0	0.0	0.0028	0.0	0.0	0.0000	0.0022
Ce	0.0614	0.0	0.0	0.0	0.0157	0.0	0.0	0.0000	0.2109
Cr	0.1728	0.0118	0.0	0.0	0.0114	0.0090	0.0090	0.0261	0.0473
Fe	0.0456	0.0	0.0986	0.0	0.0573	0.0138	0.0418	0.0195	8.5859
Mo	6.6550	6.1162	6.3868	6.4596	4.9417	5.6541	6.7542	6.9829	30.5320
Nd	0.0206	0.0	0.0	0.0	0.0070	0.0	0.0	0.0074	0.6891
P	0.0	0.0	0.0	0.0	0.2854	0.1835	0.3126	0.2480	0.9687
Si	22.284	21.374	22.328	21.980	23.261	23.030	22.469	22.469	129.29
Ti	0.3338	0.0018	0.3348	0.0010	0.0509	0.0027	0.0689	0.0087	0.2138
Zn	0.0	0.1936	0.0050	0.1592	0.0114	0.1803	0.0124	0.1877	8.8161
Zr	0.1726	0.0540	0.0740	0.0308	0.0098	0.0033	0.0433	0.0441	0.1298
Cs	0.6900	0.6000	0.6800	0.6600	0.7800	0.8200	0.7800	0.8000	5.8000
U(R), ppb	5.3	1.6500	6.2000	0.8600					
U(H), ppb	1.1	1.0	4.4000	0.5000	8.0000	8.0000	24.000	8.0000	3480.0
K	0.2578	0.0430	0.0860	0.0430	0.1808	0.1356	0.2712	0.1582	1.7179
Mg	0.0	0.0	0.0	0.0	0.0686	0.0686	0.1078	0.1176	0.8235
Na	46.146	44.562	46.646	46.116	49.202	49.899	48.379	48.632	221.4

C.1

TABLE C.1. (contd)

	Material							
	U76-68	U76-68	U76-68	Synroc-C	Synroc-C	Synroc-C	Synroc-C	Synroc-C
Size	4080 Mesh							
Fluid	Si H <sub>2</sub> O							
Volume, mL	40	40	40	40	40	40	40	40
Initial pH	8.67	8.67	8.67	8.67	8.67	8.67	8.67	8.67
Final pH	9.5	9.49	9.49	8.99	8.99	9.01	9.01	9.61
Time, days	28	28	28	56	56	56	56	90
Al	0.1626	0.3131	0.1199	0.1678	0.1317	0.1750	0.1545	0.1839
B	65.232	64.723	64.092	0.0220	0.0142	0.0104	0.0078	0.0092
Ba	0.0173	0.0614	0.0060	2.8042	0.9283	2.5006	0.5319	2.2119
Ca	0.5194	0.7570	0.3120	0.2563	0.2891	0.2221	0.2206	0.2699
Cd	0.0009	0.0033	0.0046	0.0000	0.0	0.0	0.0	0.0
Ce	0.0598	0.1783	0.0467	0.0588	0.0	0.0293	0.0	0.0270
Cr	0.0351	0.0449	0.0392	0.0174	0.0054	0.0072	0.0048	0.0068
Fe	3.2825	10.620	0.0885	0.0129	0.0	0.0259	0.0026	0.0193
Mo	31.218	29.486	27.536	5.3530	6.2611	5.7361	6.6939	7.0179
Nd	0.2226	0.7493	0.0437	0.0337	0.0000	0.0225	0.0	0.0179
P	2.1814	2.5008	1.8315	0.2176	0.2336	0.3069	0.3183	0.3036
Si	130.61	143.21	128.96	23.321	23.035	23.083	22.844	23.552
Ti	0.0777	0.2609	0.0071	0.0626	0.0	0.0886	0.0009	0.1078
Zn	4.4905	10.476	1.4218	0.0028	0.1292	0.0019	0.1167	0.0
Zr	0.0612	0.1388	0.0563	0.0	0.0	0.0	0.0	0.0130
Cs	5.6000	6.0000	5.0000	1.3000	1.1000	1.2000	1.1000	1.3000
U(R), ppb								
U(H), ppb	2720.0	3400.0	2640.0	0.0080	0.0	0.0080	0.0080	0.0500
K	1.4919	1.7405	1.6727	0.2177	0.2022	0.1711	0.2177	0.2439
Mg	0.4020	0.9804	0.2059	0.0	0.0	0.0	0.0	0.0
Na	226.91	228.87	224.44	50.980	51.689	51.379	51.556	51.634

TABLE C.1. (contd)

	Material						
	Synroc-C	Synroc-C	Synroc-C	U76-68	U76-68	U76-68	U76-68
Size	4080 Mesh						
Fluid	Si H <sub>2</sub> O						
Volume, mL	40	40	40	40	40	40	40
Initial pH	8.67	8.67	8.67	8.67	8.67	8.67	8.67
Final pH	9.61	9.60	9.60	9.87	9.87	9.87	9.87
Time, days	90	90	90	90	90	90	90
Al	0.1776	0.3241	0.2722	0.6252	0.0	0.6446	0.0
B	0.0046	0.0116	0.0081	78.942	80.907	81.335	81.023
Ba	0.8658	2.1508	0.8826	0.2025	0.0005	0.1887	0.0003
Ca	0.2658	0.2617	0.2302	1.6427	0.3891	1.5934	0.4220
Cd	0.0	0.0	0.0	0.0117	0.0	0.0117	0.0004
Ce	0.0	0.0451	0.0	0.5000	0.0087	0.4500	0.0270
Cr	0.0085	0.0074	0.0057	0.1260	0.0635	0.1260	0.0607
Fe	0.0	0.0204	0.0	16.9990	0.0472	21.046	0.0548
Mo	7.1784	7.0313	7.0580	39.7000	40.670	41.452	39.025
Nd	0.0	0.0271	0.0	2.1696	0.0227	2.1469	0.0179
P	0.2734	0.2751	0.2549	4.1362	1.4928	4.1748	1.4140
Si	23.621	23.759	23.184	143.0000	139.30	138.98	139.18
Ti	0.0	0.0956	0.0	0.4138	0.0067	0.5180	0.0063
Zn	0.0848	0.0	0.0780	19.2230	1.5199	22.173	1.6566
Zr	0.0	0.0120	0.0	0.0845	0.0058	0.1166	0.0048
Cs	1.3000	1.3000	1.3000	12.5000	6.5000	11.400	6.3000
U(R), ppb							
U(H), ppb	0.0500	0.0500	0.0500	3.9500	0.2800	4.1100	0.3000
K	0.3523	0.2710	0.1626	2.3575	1.9646	2.3033	1.9781
Mg	0.0000	0.0112	0.0	1.0900	0.1180	1.2473	0.1348
Na	52.448	51.905	51.498	282.57	278.16	287.93	276.36

(a) Results are reported in ppm unless otherwise noted.

(b) -40/+80 mesh.

TABLE C.2. MCC-3, Powder, 150°C, Silicate Water<sup>(a)</sup>

	Material								
	Synroc-C	Synroc-C	Synroc-C	Synroc-C	Synroc-C	Synroc-C	Synroc-C	Synroc-C	U76-68
Size	4080 Mesh <sup>(b)</sup>	4080 Mesh							
Fluid	Si H <sub>2</sub> O	Si H <sub>2</sub> O	Si H <sub>2</sub> O	Si H <sub>2</sub> O	Si H <sub>2</sub> O	Si H <sub>2</sub> O	Si H <sub>2</sub> O	Si H <sub>2</sub> O	Si H <sub>2</sub> O
Volume, mL	15	15	15	15	15	15	15	15	15
Initial pH	8.67	8.67	8.67	8.67	8.67	8.67	8.67	8.67	8.67
Final pH	9.03	9.03	8.89	8.89	9.0	9.0	7.72	7.72	9.81
Time, days	14	14	14	14	28	28	28	28	28
Al	0.4808	0.4614	0.6300	0.5742	0.4675	0.3701	0.3693	0.3494	0.0
B	0.1366	0.1032	0.0278	0.0196	0.1243	0.0879	0.0339	0.0163	244.27
Ba	2.3966	0.6148	2.6750	0.4726	1.3779	0.2421	3.6239	1.3543	0.0020
Ca	0.0946	0.1826	0.1318	0.1690	0.1900	0.1528	0.2514	0.4471	0.3385
Cd	0.0	0.0	0.0	0.0	0.0015	0.0	0.0	0.0	0.0023
Ce	0.0	0.0	0.0308	0.0	0.0094	0.0	0.0	0.0	0.0
Cr	0.0234	0.0168	0.0184	0.0184	0.0247	0.0147	0.0053	0.0047	1.0648
Fe	0.0	0.0	0.0	0.0	0.0251	0.0	0.0013	0.0	0.0798
Mo	7.9830	8.0682	8.1534	8.0832	6.7925	8.0990	8.1889	8.6589	122.42
Nd	0.0	0.0	0.0	0.0	0.0165	0.0	0.0	0.0	0.0
P	0.0870	0.0	0.0	0.0	0.1975	0.1309	0.2664	0.2181	8.7348
Si	24.41	23.652	23.340	22.386	23.351	23.303	23.09	22.9	309.68
Ti	0.0160	0.0010	0.0076	0.0	0.0013	0.0	0.0	0.0	0.0
Zn	0.0222	0.1170	0.0028	0.1628	0.0027	0.1115	0.0013	1.3535	0.1307
Zr	0.0232	0.0108	0.0	0.0	0.0	0.0	0.0	0.0	0.0388
Cs	1.4000	1.6000	2.3000	2.1000	2.0	2.0	2.2000	2.2	1.1000
U(R), ppb	0.0	0.8600	0.0	0.8600					
U(H), ppb	1.0	0.5000	0.5000	0.5000	8.0	8.0	15.0	8.0000	3600.0
K	0.1288	0.1718	0.2148	0.1718	0.1982	0.0	0.0	0.0152	4.2088
Mg	0.0	0.0	0.0	0.0	0.0296	0.0	0.0	0.0	0.1718
Na	47.408	46.016	46.838	45.424	51.866	53.228	51.185	50.802	716.76

C.4

TABLE C.2. (contd)

	Material								
	U76-68	Synroc-C	Synroc-C	Synroc-C	Synroc-C	Synroc-C	Synroc-C	U76-68	U76-68
Size	4080 Mesh								
Fluid	Si H <sub>2</sub> O								
Volume, mL	15	15	15	15	15	15	15	15	15
Initial pH	8.67	8.67	8.67	8.67	8.67	8.67	8.67	8.67	8.67
Final pH	9.81	9.81	9.81	9.84	9.84	9.34	9.34	9.93	10.01
Time, days	28	56	56	90	90	90	90	90	90
Al	0.0	0.7545	0.7420	0.6039	0.5586	0.4730	0.4008	0.0000	0.0
B	243.55	0.2331	0.1865	0.0890	0.0844	0.0462	0.0451	388.12	386.75
Ba	0.0005	0.5926	0.1818	1.4220	0.1488	2.4656	0.6074	0.0070	0.0215
Ca	0.5456	0.1282	0.1282	0.2151	0.1329	0.2480	0.2521	1.5865	0.6782
Cd	0.0004	0.0	0.0	0.0	0.0	0.0	0.0	0.0127	0.0120
Ce	0.0	0.0197	0.0000	0.0269	0.0				
Cr	1.0572	0.0235	0.0186	0.0165	0.0187	0.0250	0.0238	2.9078	3.2085
Fe	0.0221	0.0126	0.0013	0.0130	0.0023	0.0096	0.0146	0.0667	1.9486
Mo	122.06	7.4530	8.1128	8.4956	8.5156	8.7831	8.7229	195.84	194.81
Nd	0.0000	0.0053	0.0116						
P	8.9690	0.1809	0.2084	0.1476	0.1191	0.1275	0.0973	4.9161	7.0077
Si	271.95	26.924	26.113	24.588	23.667	24.381	23.414	242.29	318.86
Ti	0.0	0.0055	0.0	0.0027	0.0	0.0024	0.0	0.0059	0.1317
Zn	1.9395	0.0023	0.1731	0.0036	0.1352	0.0050	0.2186	3.3871	1.5700
Zr	0.0126	0.0	0.0	0.0	0.0	0.0	0.0	0.0062	0.0259
Cs	10.300	1.5000	1.3000	2.0000	1.8000	2.1000	1.8000	7.7000	9.6000
U(R), ppb									
U(H), ppb	2200.0	50.0	1000.0						3400.0
K	3.7666	0.3266	0.2799	0.3387	0.2439	2.3575	0.2710	3.5091	3.9020
Mg	0.1303	0.0060	0.0000	0.0169	0.0	0.0169	0.0	0.4326	0.2922
Na	715.36	55.675	53.814	52.584	51.294	51.464	50.31	1010.6	1018.9

(a) Results are reported in ppm unless otherwise noted.

(b) -40/+80 mesh.



APPENDIX D

LEACH TEST RESULTS FROM MCC-3 TESTS ON SYNROC-C AND 76-68 GLASS IN BRINE



TABLE D.1. MCC-3, Powder, 90°C, Brine<sup>(a)</sup>

	Material					
	Synroc-C	Synroc-C	Synroc-C	Synroc-C	U76-68	U76-68
Size	4080 Mesh <sup>(b)</sup>	4080 Mesh				
Fluid	Brine	Brine	Brine	Brine	Brine	Brine
Volume, mL	40	40	40	40	40	40
Initial pH	4.43	4.43	4.43	4.43	4.43	4.43
Final pH	3.57	3.57	3.62	3.62	5.39	5.39
Time, days	28	28	28	28	28	28
Al	0.0	0.105	0.0	0.015	0.0	0.0
B	0.924	1.223	0.492	0.686	101.19	101.49
Ba	7.269	7.257	7.476	7.482	22.427	22.487
Ca	1.165	1.412	1.147	1.342	62.542	62.665
Cd	0.0	0.006	0.0	0.012	1.497	1.515
Ce	0.856	0.683	0.683	0.681	1.022	0.681
Cr	0.117	0.144	0.081	0.099	0.153	0.189
Fe	0.054	0.012	0.018	0.018	0.108	0.048
Mo	9.535	11.975	8.951	10.012	42.872	39.531
Nd	0.462	0.462	0.394	0.575	0.739	0.639
P	0.368	0.057	0.368	0.170	0.198	0.311
Si	0.905	0.941	0.905	0.977	26.597	26.38
Ti	0.021	0.036	0.016	0.026	0.026	0.031
Zn	0.0	1.365	0.0	1.493	141.73	143.95
Zr	0.115	0.151	0.070	0.133	0.113	0.292
Cs	0.730	0.510	0.730	0.680	43.10	42.70
U	0.030	0.030	0.030	0.030	0.030	0.030

(a) Results are reported in ppm unless otherwise noted.

(b) -40/+80 mesh.

TABLE D.1. (contd)

	Material					
	U76-68	U76-68	Synroc-C	Synroc-C	Synroc-C	Synroc-C
Size	4080 Mesh					
Fluid	Brine	Brine	Brine	Brine	Brine	Brine
Volume, mL	40	40	40	40	40	40
Initial pH	4.43	4.43	4.43	4.43	4.43	4.43
Final pH	4.94	4.94	3.63	3.63	3.6	3.6
Time, days	28	28	90	90	90	90
Al	0.0	0.0	2.817	2.884	2.885	3.143
B	102.53	102.39	0.485	0.497	0.497	0.474
Ba	22.487	22.547	6.384	6.509	6.280	6.269
Ca	62.63	62.383	4.042	4.233	3.987	4.124
Cd	1.521	1.480	0.154	0.173	0.171	0.182
Ce	1.024	0.510	1.700	1.608	1.789	1.881
Cr	0.144	0.126	1.418	1.435	1.413	1.441
Fe	0.036	0.042	0.594	0.598	0.717	0.613
Mo	46.811	44.543	7.870	7.970	7.796	7.910
Nd	0.752	0.521	1.613	1.661	1.701	1.705
P	0.028	0.000	7.648	7.414	7.850	7.481
Si	25.954	25.62	5.916	5.985	6.054	6.054
Ti	0.026	0.010	0.121	0.125	0.125	0.129
Zn	141.98	143.54	0.170	1.782	0.1834	1.919
Zr	0.131	0.193	0.192	0.168	0.178	0.168
Cs	43.30	43.80	1.500	1.500	1.500	1.500
U	0.030	0.030	0.050	0.050	0.050	0.050

TABLE D.2. MCC-3, Powder, 150°C, Brine<sup>(a)</sup>

	Material					
	Synroc-C	Synroc-C	Synroc-C	Synroc-C	U76-68	U76-68
Size	4080 Mesh <sup>(b)</sup>	4080 Mesh				
Fluid	Brine	Brine	Brine	Brine	Brine	Brine
Volume, mL	15	15	15	15	15	15
Initial pH	4.43	4.43	4.43	4.43	4.43	4.43
Final pH	4.04	4.04	4.11	4.11	4.34	4.34
Time, days	28	28	28	28	28	28
Al	0.316	0.0	0.0	0.0	0.007	0.0
B	2.520	2.564	1.416	1.744	255.21	254.02
Ba	16.162	16.072	13.533	13.530	55.428	54.919
Ca	4.748	4.678	4.854	5.207	153.49	151.90
Cd	0.018	0.0	0.024	0.0	3.703	3.641
Ce	0.683	0.340	0.680	0.337	1.355	0.838
Cr	0.116	0.126	0.126	0.072	0.153	0.135
Fe	0.936	0.156	0.444	0.168	0.174	0.108
Mo	11.975	11.723	12.173	11.988	10.1714	9.866
Nd	0.458	0.285	0.634	0.394	1.813	1.631
P	0.510	0.340	0.510	0.680	1.302	0.028
Si	1.484	1.339	5.356	5.138	73.675	70.997
Ti	0.026	0.010	0.031	0.010	0.036	0.010
Zn	0.0	1.686	0.0	2.829	354.02	352.09
Zr	0.133	0.079	0.088	0.061	0.148	0.121
Cs	1.400	1.400	1.500	1.700	117.0	114.0
U	0.030	0.030	0.030	0.030	0.030	0.030

(a) Results are reported in ppm unless otherwise noted.

(b) -40/+80 mesh.

TABLE D.2. (contd)

	Material					
	U76-68	U76-68	Synroc-C	Synroc-C	Synroc-C	Synroc-C
Size	4080 Mesh					
Fluid	Brine	Brine	Brine	Brine	Brine	Brine
Volume, mL	15	15	15	15	15	15
Initial pH	4.43	4.43	4.43	4.43	4.43	4.43
Final pH	4.35	4.35	3.81	3.81	4.44	4.44
Time, d	28	28	90	90	90	90
Al	0.004	0.0	3.1690	2.929	2.9280	2.9370
B	249.55	246.12	0.5780	0.509	0.4970	0.4620
Ba	53.72	53.15	13.945	13.44	14.709	14.540
Ca	149.25	146.78	10.632	10.851	9.0420	9.5220
Cd	3.588	3.529	0.1890	0.185	0.1630	0.1770
Fe	1.009	0.669	2.1500	1.789	1.6070	1.6080
Cr	0.260	0.233	1.4410	1.441	1.4520	1.4470
Fe	0.186	0.102	0.6100	0.613	0.5980	0.6020
Mo	10.489	10.277	10.792	10.604	10.738	10.477
Nd	1.745	1.523	1.9320	1.752	0.1754	1.7110
P	7.347	0.198	0.057	7.967	7.4810	7.6320
Si	73.711	72.77	8.587	8.264	8.1260	7.9880
Ti	0.031	0.010	0.1410	0.133	0.1250	0.1170
Zn	345.06	340.49	0.1526	3.787	0.1778	3.9116
Zr	0.193	0.220	0.1820	0.168	0.1680	0.1580
Cs	122.0	112.0	1.5000	1.600	1.5000	1.6000
U	0.030	0.030	0.0500	0.050	0.0500	0.0500

D.4

DISTRIBUTION

<u>No. of Copies</u>		<u>No. of Copies</u>
	<u>OFFSITE</u>	
30	DOE Technical Information Center	A. T. Clark Division of Fuel Material Safety Nuclear Regulatory Commission Washington, DC 20555
5	Geologic Repository Division DOE Office of Civilian Radioactive Waste Management Forrestal Building Washington, DC 20585 ATTN: J. W. Bennett, RW-20 C. R. Cooley, RW-4 M. W. Frei B. C. Rusche, RW-1 R. Stein, RW-23	W. J. Dircks Office of the Executive Director for Operations Mail Station 6209 Nuclear Regulatory Commission Washington, DC 20555
3	DOE Office of Defense Waste & Byproducts Management GTN Washington, DC 20545 ATTN: R. K. Hensser J. E. Lytle, DP-12 R. D. Walton, Jr., DP-123	2 Environmental Protection Agency Office of Radiation Programs 401 M Street, S.W. Washington, DC 20460 ATTN: D. Egan G. L. Sjoblom
7	DOE Office of Terminal Waste Disposal & Remedial Action GTN Washington, DC 20545 ATTN: J. E. Baublitz, NE-24 J. A. Coleman, NE-25 D. J. McGoff, NE-23 T. W. McIntosh, NE-25 W. R. Voigt, NE-20 H. F. Walter, NE-25 J. B. Zorn, NE-25	3 DOE Albuquerque Operations Office P.O. Box 5400 Albuquerque, NM 87185 ATTN: K. A. Carlson M. H. McFadden J. McGough
	M. J. Bell Division of Nuclear Materials Safety & Safeguards Mail Station 881-SS Nuclear Regulatory Commission Washington, DC 20555	P. G. Hagan Joint Integration Office Bldg. 3, 2nd Floor 2201 San Pedro N.E. Albuquerque, NM 87110
		E. Maestas DOE West Valley Operations Office P.O. Box 191 West Valley, NY 14171

No. of  
Copies

No. of  
Copies

3 DOE Idaho Operations Office  
550 Second Street  
Idaho Falls, ID 83401  
ATTN: M. J. Barainca  
J. P. Hamric  
J. B. Whitsett

F. T. Fong  
DOE San Francisco Operations  
1333 Broadway  
Oakland, CA 94612

M. R. Jugan  
DOE Oak Ridge Operations Office  
P.O. Box E  
Oak Ridge, TN 37830

S. A. Mann  
DOE Chicago Operations Office  
9800 South Cass Avenue  
Argonne, IL 60439

J. O. Neff  
DOE National Waste Program  
Office  
505 King Avenue  
Columbus, OH 43201

W. J. Brumley  
DOE Savannah River Operations  
Office  
P.O. Box A  
Aiken, SC 29801

D. L. Vieth  
DOE Nevada Operations Office  
P.O. Box 14100  
Las Vegas, NV 89114

2 Argonne National Laboratory  
9700 South Cass Avenue  
Argonne, IL 60439  
ATTN: M. J. Steindler  
L. E. Trevorrow

C. S. Abrams  
Argonne National Laboratory  
P.O. Box 2528  
Idaho Falls, ID 83401

2 Battelle Memorial Institute  
Office of Crystalline Repository  
Development  
9800 South Cass Avenue  
Argonne, IL 60439  
ATTN: W. J. Madia  
B. D. Shipp

3 Battelle Memorial Institute  
Project Management Division  
505 King Avenue  
Columbus, OH 43201  
ATTN: W. A. Carbeiner/  
S. H. Basham  
J. F. Kircher  
B. Rawles

F. Holzer  
Lawrence Livermore National  
Laboratory  
University of California  
P.O. Box 808  
Livermore, CA 94550

D. T. Oakley, MS 671  
Los Alamos Scientific Laboratory  
P.O. Box 1663  
Los Alamos, NM 87544

6 Oak Ridge National Laboratory  
P.O. Box Y  
Oak Ridge, TN 37830  
ATTN: J. O. Blomeke  
W. D. Burch  
R. T. Jubin  
L. J. Mezga  
T. H. Row

No. of  
Copies

No. of  
Copies

5 Sandia Laboratories  
P.O. Box 5800  
Albuquerque, NM 87185  
ATTN: D. R. Anderson  
J. F. Ney  
R. W. Lynch  
W. Weart  
Technical Library

J. R. Berreth  
Westinghouse Idaho Nuclear  
Co., Inc.  
P.O. Box 4000  
Idaho Falls, ID 83401

7 E. I. du Pont de Nemours  
Company  
Savannah River Laboratory  
Aiken, SC 29801  
ATTN: M. D. Boersma  
J. G. Glasscock  
E. J. Hennelly  
C. M. Jantzen  
J. R. Knight  
M. J. Plodinec  
C. T. Randall

E. A. Jennrich  
EG&G Idaho  
P.O. Box 1625  
Idaho Falls, ID 83415

V. Ricks  
EG&G  
1580 Sawtill  
P.O. Box 1680  
Idano Falls, ID 83415

G. W. Meyers  
Atomics International Division  
Rockwell International  
8900 DeSoto Avenue  
Canoga Park, CA 91304

T. H. Pigford  
Department of Nuclear  
Engineering  
University of California  
Berkeley, CA 94720

M. E. Spaeth  
Science Applications, Inc.  
2769 South Highland  
Las Vegas, NV 89109

J. F. Strahl  
Weston  
2301 Research Boulevard  
Third Floor  
Rockville, MD 20850

R. Williams  
Electric Power Research  
Institute  
3412 Hillview Avenue  
P.O. Box 10412  
Palo Alto, CA 94304

5 West Valley Nuclear Services  
Company  
P.O. Box 191  
West Valley, NY 14171  
ATTN: C. C. Chapman  
J. C. Cwynar  
J. L. Knabenschuh  
J. E. Krauss  
J. M. Pope

J. W. Bartlett  
The Analytic Sciences  
Corporation  
6 Jacob Way  
Reading, MA 01867

W. A. Freeby/J. L. Jardine  
Bechtel National, Inc.  
P.O. Box 3965  
San Francisco, CA 94119

No. of  
Copies

No. of  
Copies

Librarian  
Westinghouse Electric  
Corporation  
Technical Library  
P.O. Box 2078  
Carlsbad, NM 88220

L. L. Hench  
Department of Materials Science  
& Engineering  
University of Florida  
Gainesville, FL 32611

J. L. Larocca, Chairman  
Energy Research & Development  
Authority  
Empire State Plaza  
Albany, NY 12223

R. G. Post  
College of Engineering  
University of Arizona  
Tucson, AZ 85721

10 Rockwell Hanford Operations

R. N. Gurley  
H. E. McGuire  
J. W. Patterson  
R. D. Prosser  
I. E. Reep  
R. J. Thompson  
T. B. Venziano  
D. D. Wodrich  
R. D. Wojtasek  
File Copy

UNC United Nuclear Industries

T. E. Dabrowski/W. J. Kyriazis

2 Westinghouse Hanford Company

R. E. Lerch  
J. D. Watrous

59 Pacific Northwest Laboratory

W. J. Bjorklund  
H. T. Blair  
W. F. Bonner  
D. J. Bradley  
R. A. Brouns  
L. R. Bunnell  
L. L. Burger/L. A. Bray/  
R. D. Scheele  
H. C. Burkholder  
J. R. Carrell  
R. D. Dierks  
S. K. Edler  
R. W. Goles  
M. S. Hanson  
H. A. Haerer  
L. K. Holton

ONSITE

12 DOE Richland Operations Office

J. H. Anttonen  
E. A. Bracken  
G. J. Bracken  
C. R. DeLannoy  
R. D. Izatt  
N. T. Karagianes  
M. J. Plahuta  
J. L. Rhoades  
M. W. Shupe  
J. J. Sutey  
J. D. White  
J.K.W. Wukelik

No of  
Copies

J. H. Jarrett  
D. E. Knowlton  
S. S. Koegler  
M. R. Kreiter  
W. W. Laity  
L. T. Lakey/K. M. Harmon  
J. M. Latkovich  
J. L. McElroy  
G. L. McVay  
J. E. Mendel/M. D. Merz/  
G. B. Mellinger  
J. E. Minor  
L. G. Morgan  
D. R. Montgomery

No. of  
Copies

T. R. Myers  
R. D. Peters  
M. E. Peterson  
A. M. Platt/R. E. Nightingale  
J. A. Powell  
W. A. Ross  
K. J. Schneider  
P. A. Scott  
J. W. Shade (10)  
D. H. Siemens  
G. L. Tingey/G. A. Jensen  
Publishing Coordination (2)  
Technical Information (5)

